Biochar-based thin-layer capping of contaminated sediment in Burefjärden, northern Sweden

Assessment of biochar mixed into four structural materials for preventing release of trace elements from sediment to water

Nathalie Pantzare

Natural Resources Engineering, master's
2021

Luleå University of Technology
Department of Civil, Environmental and Natural Resources Engineering

Acknowledgements

This thesis compiles the final part within a master's degree in Natural Resources Engineering at Luleå University of Technology. The thesis was conducted during the spring of 2021.

Throughout the writing process I have received a lot of support and assistance. I would first like to thank my supervisor, Christian Maurice, whose knowledge and feedback provided has been greatly appreciated. Furthermore, I wish to show my gratitude to Anders Widerlund, whose expertise within the subject of geochemistry has been a valuable resource throughout the project.

In addition, I would also like to thank my family for all the support during my studies. Finally, I could not have completed this thesis without the help of my friends, who provided great discussions and lots of laughs during this project. Thank you all!

Luleå, June 2021
Nathalie Pantzare

Abstract

Coastal areas around the world have been recognized as largely impacted by anthropogenic activities resulting in pollution of marine sediments. In Sweden, surveys conducted along the coastline of the Bothnian Bay have identified a total area of about 29 km^2 as fiber rich sediments. In the Bureå sea area near Skellefteå vicinity, Västerbotten county, elevated levels of mercury (Hg), methyl-Hg, arsenic (As), copper (Cu), lead (Pb), cadmium (Cd), zinc (Zn) and polycyclic aromatic hydrocarbons (PAH) have been classified and believed to be mainly affected by emissions from a pulp and paper industry formerly active on a nearby headland.

Contaminants in sediments are of concern as continuous dispersion can adversely affect the benthic community. To isolate contaminants and reduce their bioavailability, in-situ thin-layer capping using an active material is one suitable approach. This type of remediation method, using biochar mixed with bentonite clay will be implemented on a pilot scale in the sea area outside of Bureå in the spring of 2021. However, bentonite is a relatively expensive material yielding a need to further develop the selection of capping materials suitable to aid in the deposition of biochar in an active thin-layer cap.

In this thesis, biochar-based thin layer caps mixed with bentonite clay, rock dust of two grain sizes and a concrete-based slurry was evaluated on their physicochemical properties and efficiency for preventing release of trace elements from sediment to the overlying water. This was conducted by a laboratory column experiment where four set ups were performed: (1) no capping for sediment control, (2) only capping material for material control, (3) sediment mixed with biochar and (4) sediment capped with each material mixed with biochar. Three times during an 8-week test period, 60 mL of the overlying water in the columns was extracted and sent for trace element analysis.

The experimental set up revealed that the capping layers effectively prevent release of trace elements trough the sediment to the overlying water. The concrete slurry showed suitable settling properties and negligible loss of biochar in the set-up of the columns. Also, the biochar+concrete slurry thin-layer cap displayed the highest efficiency for preventing and/or delaying release of As, P, Cu, Fe, Mn and SO_4.

Table of Contents

1 Introduction

Metal contamination of marine sediments is a worldwide environmental issue and is, along the coastline of the Nordic countries, mainly an impact from historical industrial activities (Peng et al, 2009; Jersak et al, 2016a). In Sweden, sediments in inland and/or coastal waters have been recognized as contaminated in 19 out of 21 counties according to investigations carried out in 2016 (Olsen et al, 2019). Sediments play an important role for storing and transporting potentially toxic elements, as they can serve as both a sink and a source for contaminants that enter the aquatic system. Changes in the sediment's physicochemical characteristics may cause bound metals to re-enter the overlying water body and become bioavailable, posing a threat to all organisms in the food chain (Naturvårdsverket 2003; Zhang et al, 2016). In later years, regulations to reduce pollution levels have resulted in development of globally accepted technologies for remediating contaminated sediments (Lehoux et al, 2020). These techniques can be divided into: (1) *ex situ* treatments by dredging or excavating the sediments, and (2) *in situ* treatments using passive or active capping. Selection of remediation methods is usually based on site-specific assessments, including the potential risk of the site and the cost (Zhang et al, 2016). Dredging followed by ex situ treatment has been one of the most applied methods to date. However, this technique generally results in high costs, occupation of land areas and resuspension of contaminants during dredging in comparison to the in-situ capping technique which is considered to be less environmentally disruptive and more cost-efficient, in particular when using an active capping material (Lehoux et al, 2020; Zhang et al, 2016). Hence, this type of approach has gained a lot of interest in the last decade and can be beneficially applied to contain the contaminants and reduce their bioavailability (Naturvårdsverket, 2003).

Knowledge about contaminated sites on land is generally greater and the techniques further developed than those in marine environments (Naturvårdsverket, 2020a). Thus, an initiative to improve knowledge of cost-efficient management of contaminated sediments in lakes and coastal areas in Sweden have been assigned to the Swedish Environmental Protection Agency (SEPA) in collaboration with the Geological Survey of Sweden (SGU), Swedish Agency for Marine and Water Management (SwAM), the County Administrative Boards and the Swedish Geotechnical Institute (SGI) by the Swedish Government in 2019 (Regeringen, 2019). According to Regeringen (2019), this assignment includes "*...i.e., efforts to gain better knowledge about the distribution of polluted sediment areas, the risk of spreading environmental toxins and various alternative measures*".

Investigations conducted in the coastal areas show that both fiber banks and fiber rich sediments are prevalent along the Swedish coastline. In the sea area near Bureå, Skellefteå, a total area of 254 000 m^2 has been classified as fiber rich sediments with elevated concentrations of mercury (Hg), methyl-Hg, arsenic (As), copper (Cu), lead (Pb), cadmium (Cd), zinc (Zn) and polycyclic aromatic hydrocarbons (PAH). One major source of contribution is believed to be historical releases of fiber waste from the pulp and paper industry that was active on a nearby headland from 1928 to 1992 (SGU, 2016). One alternative for managing the contaminated sediment at this site would be to place a thin-layer cap of biochar on top of the sediment in order to isolate, degrade and immobilize the contaminants. This type of active thin-layer capping approach has been implemented in some full- and pilot scale projects in e.g., the USA and Norway but has not yet been applied in the field in Sweden (Jersak et al, 2016b; Olsen et al, 2019). Furthermore, implementation and research of biochar as an active material in environmental management of contaminated sediments are limited to this day (Yang et al, 2020) and therefore a small-scale project will be implemented in the sea area outside of Bureå to evaluate the viability of this approach. Bentonite clay will be mixed with biochar to aid in deposition as biochar usually has a low density in the range of 10^1-10^2 $kg \cdot m^{-3}$ (Joseph et al, 2015; Yang et al, 2020). However, bentonite is a relatively expensive material (approximately 2-3 SEK/kg depending on amount and quality) and thus, this thesis aims to further develop the selection of capping materials suited to be mixed with biochar. Rock dust and a concrete-based slurry are possible alternative materials. This was conducted by a laboratory bench-scale experiment especially focused on sediment pore water and overlying water column geochemistry to explain fluxes and transport of contaminants through the different capping materials.

1.1 Aim and objective

This master thesis was performed with the primary objective to evaluate the technical and chemical performance of biochar-based thin-layer caps mixed with four different structural materials; bentonite clay, concrete slurry and rock dust of two different particle sizes. The assessment was carried out by the use of a bench-scale column experiment where fiber rich sediment collected near Bureå, Skellefteå, was covered with the different capping materials and the pH, EC and trace element concentrations in the overlying water column were analysed. Thus, the focus of this study was to assess the release of contaminants from sediment to water by answering the following research questions:

- What are the physicochemical properties of the different materials and which material is most suitable to aid biochar in deposition?
- How do the different capping materials affect pH, EC and concentrations of trace elements in the overlying water column?
- How are substances with different chemistry, e.g., cations Cu and Zn compared to the anions As and P, affected by the capping materials? Are there any noticeable differences?

1.2 Limitations

This study is limited to a physicochemical assessment of different thin-layer caps with reference to inorganic trace elements, mainly As, Hg, Cd, Zn, Pb and Cu. Fluxes and transport of organic pollutants as well as behaviors and effects on marine biota will not be analyzed and further considered. This master thesis may also have limitations in the laboratory set up, as time and water fluxes does not fully reflect real field conditions.

2 Theoretical background

2.1 Historical view of the site

The sea area outside of Bureå is located in the Bothnian Bay, the northernmost part of the Gulf of Bothnia, with a low salinity of about 2-4 PSU (Kautsky & Kautsky, 2000). It is an enclosed area with no tide, and it is ice covered during the winter. In the northern part of the area, the Skellefteå River has its outlet and in the southwest, the Bureå River flows into the Burefjärden sea area (Figure 1). The sediment in Burefjärden displays elevated concentrations of organic and inorganic compounds. Several potential sources of pollution have been investigated in the nearby areas. During the years 1928 to 1992, a pulp- and paper industry (former Bure AB) was active in the Bureå area. Between 1948-1964 they used a Hg-based chemical for preserving the pulp (Skellefteå kommun, 2020a). In Örviken and Klemensnäs, pulp and paper production factories have been active until the 1990s contributing to release of As and metals in the Skellefteå River from pyrite ash and phenyl-Hg rich waste (Geo Innova, 2008; Skellefteå kommun, 2020b).

The Skellefteå area is characterized by a mineral rich sulfide ore belt and large-scale mining production. The area has shown higher background concentrations of metals, in particular As, than the average concentrations in Sweden (Länsstyrelsen, n.d.). The currently active Rönnskärsverken smelter in Skelleftehamn about 5 km north of the Bureå area is a large contributor for release of e.g. As, Cu, Pb and Zn (Naturvårdsverket, 2020b).

Fig 1. Skelleftebukten and nearby areas. Areas contributing to potential sources of pollution are marked with red squares. The sediment studied in this investigation is located close to the Bureå contaminated site.

2.1.1 Previously conducted investigations at the site

SGU (2016) has conducted a classification survey of fiber banks and fiber rich sediments caused by pulp and paper industries located along the Bothnian Bay coastline. In Bureå, an area of 18 000 m^2 has been classified as fiber banks and a total area of 254 000 m^2 as fiber rich sediments. The fiber banks and sediments have no to little overlying sediment due to the area being exposed to the open sea which causes resuspension preventing the natural accumulation of sediments. Samples in and around Burefjärden show that the upper part of the sediments predominantly consist of postglacial clay and silt (mainly a particle size of <60 µm) and that it contains high levels of environmental toxins in the form of both organic and inorganic contaminants. Levels of As, Hg, Cd, Cu, Pb and Zn have been found to largely deviate from comparative values in the area. SGU (2016) also reported high concentrations of methyl-Hg and that the most elevated levels of As, Hg and Pb occur at the sampling point furthest away from the coastline, indicating that the contaminants could derive from other sources in the nearby Skellefteå area.

An investigation carried out by Geo Innova (2008) in the Klemensnäs area about 15 km from Burefjärden, mentions that pollution of As from a previously active pulp industry has been detected in the groundwater and that probable migration to the Skellefteå River can be expected. In the classification survey performed by SGU (2016) it is also stated that sediment in the Örviken area, about 5 km from Bureå, contains extremely high levels of methyl-Hg and heavy metals. Furthermore, SGU (2016) writes that organic pollutants are generally not elevated, except for PAH which displays higher levels. A complementary survey conducted by Ramboll (2019a) also states that the sea area outside of Bureå is heavily affected by heavy metals and PAH. Sampling campaigns show that levels of As, Hg, Cd, Pb, Cu and Zn are most elevated in the northern part of the area and generally decline to the south. Average and maximum values from 34 sampling points around the Bureå sea area are compiled in Table 1. Furthermore, Ramboll (2019a) describes that results from a biological investigation show no elevation in uptake of Hg in the bottom fauna and that no negative effects on fish have been found in the Burefjärden area. However, they also state that the conditions for benthic and bottom-dwelling pelagic organisms to flourish in this environment are limited.

Table 1. Element concentrations ($mg \cdot kg^{-1}$ dry weight) in sediment from a sampling campaign in Burefjärden performed by Ramboll (2019a). Guide value is “class V”, very high levels, from Naturvårdsverkets assessment criteria for metals in marine sediment (Naturvårdsverket, 1999).

Element	Average value	Maximum value	Guide value
As	424	2460	>45
Hg	4.9	18	>1
Cu	142	615	>80
Cd	3.2	13	>3
Pb	232	1120	>110
Zn	254	935	>357

2.2 Heavy metal contamination in sediments

Sediments at the bottom of the world's oceans, lakes and rivers play a significant role for the aquatic environment as they act as both a sink and a potential source for contaminants. The potential risk of the sediment depends on contaminant migration and bioavailability (Severin et al, 2018). Contaminants can accumulate at relatively large distances from the original source and metals that enter the water can get adsorbed onto the sediment resulting in decreased mobility and availability (Severin et al, 2018; Wang et al, 2018). Divalent cations such as Cu(II), Pb(II), Zn(II), Cd(II) are pollutants commonly found in sediments and their distribution can cause high concentrations in sediment pore water and in the overlying water body. The metals bound in sediment can be released into the water column through pore water diffusion and resuspension and enter the food chain by becoming more mobile and available for benthic organisms (Azcue et al, 1998; Lehoux et al, 2020; Yang et al, 2020). Environmental processes that cause metals to re-enter the water are e.g., storms and waves, changes in bottom currents, post-glacial land rise and human activities such as shipping and dredging (Severin et al, 2018).

To assess the pollution levels of metals in sediments, guideline values can be used. The most accurate assessment would be to consider site specific guideline values, as background levels can vary locally. However, if no site-specific values are available, regional or national background levels can be used to assess the potential risk of the site. This is usually the case for evaluating marine sediments. In Sweden, the Swedish EPA has developed some guideline values for assessment of metals in marine sediment, which are based on reference values (background levels) for metals in the whole of Sweden (Naturvårdsverket, 1999). Some contaminants in sediment are more hazardous than others. Due to its toxicity and mobility, Hg is considered one of the most harmful contaminants. Also, inorganic Hg can convert into organometallic methyl-Hg resulting in bioaccumulation and increasing toxicity (Wang et al, 2018). Common forms of As are As(III) and As(V) with arsenite (AsO_3^{3-}) and arsenate (AsO_4^{3-}) being the most toxic and prevalent forms in water and sediment (O´day, 2006; Wang et al, 2018).

2.2.1 Partitioning and distribution of heavy metals in sediments

To understand and anticipate how contaminants move in sediments, the distribution and partitioning of trace elements are of importance. Heavy metals in sediment are generally distributed as soluble ions, colloids in pore waters and solid sedimentary phases. Sediment characteristics such as pH, redox conditions, particle size, particle distribution and presence of solid-phase compounds such as clay minerals, acid volatile sulfides (AVS), organic matter (OM) and oxides/hydroxides heavily influence the metal partitioning in the sediment (Peng et al, 2009; Zhang et al, 2014). In other words, accessibility and favorable conditions of adsorption, precipitation and/or complexation mainly controls the distribution and retention of heavy metals and changes in sediment characteristics can result in release of sediment-bound metals to the overlying water (Bourg & Loch, 1995; Peng et al, 2009).

2.2.2 Redox and pH

Redox conditions and pH in both sediment and water control the heavy metal distribution between the solid and aqueous phase, and thus influence the metal mobility (Peng et al, 2009). pH is measured on a scale of 0-14 where <7 is acidic and >7 is considered to be alkaline. A more acidic environment generally enhances the mobility of heavy metals and thus increases the release of metals from sediment while an alkaline environment benefits adsorption and precipitation of trace elements (Zhang et al, 2014). When pH is decreased in the sediment, more H^+ will become available and compete with metal cations for ligands which results in a decreased adsorption capacity and subsequently an increase in heavy metal mobility (Peng et al, 2009). This can be even more enhanced in sediments rich in OM and AVS as the degradation and oxidation releases H^+ and decreases the pH even further (Peng et al, 2009).

Redox potential (Eh) is a measurement used to characterize a system's reducing and oxidizing capacity, measured in millivolts (mV). Sediments are normally depleted in O_2 as the exchange with oxygenated waters are minimal. The vertical profile of sediments can therefore be divided into three zones: (1) the oxic zone where oxygen is present as oxidant, (2) the suboxic zone where nitrate, manganese and iron act as oxidants and (3) the anoxic zone where sulfate is reduced, sulfide is present and methanogenesis can occur. With increasing Eh in sediment, oxidation of sulfides will increase and promote release of sulfide-bound heavy metals. Mercury (Hg), iron (Fe) and manganese (Mn) are audibly affected by redox conditions in both sediment and water (Naturvårdsverket, 2003). Consequently, disturbance and oxidation of sediments should be avoided to keep heavy metals adsorbed and bound as complexes (Peng et al, 2009). Usual Eh values in oxidized water (>1 mg O_2 l^{-1}) are 300-500 mV and in reduced sediment below 100 mV (Søndergaard, 2009). Negative Eh values indicate fine and OM-rich sediments where Fe(II), reduced Mn, hydrogen sulfide (H_2S) and organic compounds are present. Depending on their redox behavior, the trace element mobility may also be affected. Additionally, fiber rich sediments caused by industrial activity are common along coastlines worldwide and generally result in oxygen deprived seabeds yielding inhabitable conditions for benthic organisms and plants.

The effect of pH and redox on the mobility of heavy metals, such as Cu, Zn, Pb and Cd, is similar as they all are present as divalent cations or compounds with the same properties (Wang et al, 2018). They are normally released when sediment conditions change from near neutral and reduced to moderately acid and oxidizing conditions (Gambrell et al, 1991). However, this is not the case for all contaminants. The speciation of arsenic (As(III) vs As(V)) is regulated by redox potential and pH, and anionic forms of As are more likely to be mobilized in alkaline environments in both oxidizing and reducing conditions (Wang et al, 2018).

2.2.3 Influences of acid volatile sulfides and organic matter

Acid volatile sulfides (AVS) can form in anaerobic sediments by sulfate reducing bacteria (SRB) and form solid phases with metal ions via substitution of divalent metals (Me^{2+}) and Fe(II). Furthermore, organic matter also has a significant effect on heavy metal solubility and mobility in sediment. Sediment fractions of <63 μm are the most influential on adsorption and transportation of heavy metals as their specific surface area is larger. In marine sediment, humic substances are an important trace metal carrier, meaning that a sediment with a substantial concentration of humus will have an elevated metal content (Zhang et al, 2014).

2.3 Transport of heavy metals in sediments

Transport of contaminants in sediment is mainly promoted by bioturbation, particle resuspension, submarine groundwater discharge (SGD), gas transport through the pore water column, advection, adsorption and diffusion (Bourg & Loch, 1995; Ramboll 2019a). Adsorption and precipitation have a significant impact on the retention of heavy metals while advection and diffusion are controlled by dissolved complexes (Bourg & Loch, 1995). For sediment covered with a capping layer, the movement of contaminants from sediment to the cap and into the overlying water column are significantly controlled by diffusion fluxes and advective flow (Zhang et al, 2016). However, for a fine-grained sediment the advection flow is slow ($<0.1\ \mathrm{m \cdot year^{-1}}$) making the diffusion fluxes more dominant (Naturvårdsverket, 2003).

2.3.1 Bioturbation and gas transport

Bioturbation is the reworking of sediment by benthic organisms. This changes the physicochemical properties of the sediment and affects pore water transport. Bioturbation mainly occurs in the upper 5 cm of marine sediments and is influenced by the number of species as well as the population of organisms (Naturvårdsverket, 2003). The movement of sediments caused by bioturbation also affects potential capping materials and can increase the release of heavy metals into the overlying water (Yang et al, 2020). Transport of pollutants through gas build up is also a significant process that occurs in marine sediment. Fiber rich sediments are particularly prone to gas production (e.g., CH_4, H_2S) resulting in transport of dissolved substances through the pore water column causing changes in sediment composition and element mobility (Naturvårdsverket, 2003; Zhang et al, 2016).

2.3.2 Adsorption

Retention of contaminants onto sediment as well as a thin-layer cap is dependent on the sorption capacity. Adsorption is a process that occurs when a solid substance attracts molecules of liquid and gas phase onto its surface (Artioli, 2008). This process can arise by two types of bindings: physical adsorption (physisorption) by the relatively weak multilayered Van der Waals force and chemical adsorption (chemisorption) by monolayered chemical bonds (Dabrowski, 2001). Due to its weaker binding, physisorption is relatively easily reversible and can therefore also contribute to the release of substances from a surface. Adsorption is affected by temperature (Artioli, 2008) and the relation between the distribution of the adsorbate on the adsorbent and its concentration in the fluid at a constant temperature is described by so-called adsorption isotherms. The most commonly used isotherm equations are Langmuir and Freundlich (Dabrowski, 2001). Langmuir is used for monolayer adsorption and is the most commonly used model when determining sorption of metal contaminants on biochar (Thomas, 2020). The Langmuir equation is written as:

$$qi = \frac{(K_L \cdot C_{max} \cdot c_i)}{(1+K_L \cdot c_i)} \tag{1}$$

where q_i and c_i is the solid phase concentration ($mg \cdot g^{-1}$) and liquid phase concentration ($mg \cdot L^{-1}$) respectively. K_L is the Langmuir's adsorption constant and C_{max} is the maximum adsorption capacity. Adsorptive processes are important when remediating contaminated sites, particularly when using an active sorbent such as activated carbon or biochar. Adsorption of heavy metals onto biochar is believed to be mainly regulated by the biochar's ability of electrostatic attraction (affinity) and adsorption capacity (Thomas et al, 2020; Yang et al, 2020).

2.3.3 Diffusion

When adding a capping layer on top of a sediment surface, the diffusion fluxes are altered as the diffusion gradient increases with the layer thickness. The basis of this process is a concentration gradient and movement of molecules that lead to the diffusion of substances from higher to lower concentrations. Sediment porosity and the degree of saturation of the sediment affects the diffusion of substances in sediments (Naturvårdsverket, 2003). Diffusion is described by Fick's first law which states that the diffusion flux J ($\mu g/cm^2/year$) is proportional to the concentration gradient ($\Delta C/\Delta Z$), the material porosity Ø and diffusion coefficient D:

$$J = -\emptyset \cdot D \cdot \frac{\Delta C}{\Delta Z} \tag{2}$$

2.4 Remediation techniques for contaminated sediments

To prevent contaminant transport through the sediment to the surrounding environment, different methods for managing contaminated sites have been developed. Which method to apply is usually determined by a site-specific risk assessment where several parameters, such as the needed risk reduction rate, type and level of pollution, sediment characteristics and the cost is evaluated for the site (SGF, 2020). According to Olsen et al (2019), dredging followed by ex situ treatment and isolation using different capping materials are the historically most implemented methods. Other approaches include monitored natural recovery (MNR), enhanced monitored natural recovery (EMNR), in situ treatment and thin-layer capping techniques using active materials (SGF, 2020). In recent years, the approach has shifted more towards the latter, as it is considered to be less disruptive and more cost-effective in comparison to the previously most implemented methods (Olsen et al, 2019).

2.4.1 Ex-situ methods

One of the most commonly used techniques to date, is dredging of the contaminated sediments followed by treatment ex-situ. The basics of the approach is to remove the contaminated sediments from the site, either by excavation, suction or freezing, in order to dewater and treat the sediments. This is usually followed by disposal on a landfill. The ex-situ approach is suitable for most contaminants and for sites exposed to erosion and with no natural sedimentation (SGF, 2019). Even though this approach has been widely implemented and has a high commercial availability (SGF, 2019) some drawbacks have been recognized, such as (1) the high cost, especially when managing larger contaminated areas, (2) not all contaminants can be removed by dredging resulting in long term exposure or re-suspension of contaminants to the water body (Zhang et al, 2016), and (3) the treatment of the dredged sediments is often extensive and also occupies land area (Lehoux et al, 2020).

2.4.2 In-situ methods

Monitored natural recovery (MNR) is an approach where physical, chemical and biological recovery processes are monitored at a site. This method is suitable at sites where deposition of new sediment is naturally occurring and where the amount of pollutant migration by different transport mechanisms is minimal. Monitoring of the site should be ongoing for an extended period of time to ensure that the elevated concentrations are decreasing (SGF, 2020). When the natural sedimentation process is aided by a thin layer of a passive, conventional material the method is called enhanced monitored natural recovery (EMNR). The requirements for long-term monitoring are the same for EMNR and MNR, with the exception of the enhanced sedimentation rate caused by the thin material cover (SGF, 2020).

Treatment in situ is a method where different types of treatment agents (chemical, biological, bio-chemical, stabilizers/solidifiers) are mechanically mixed or injected near the surface of the contaminated sediments in order to reduce the bioavailability of the contaminants (SGF, 2018). However, this approach is not widely used as it has been recognized to have significant drawbacks such as disruption of the benthic ecosystem, limitations in control of the process and application with regards to water depth (Jersak et al, 2016a). Another in-situ approach is the isolation capping technology, where one or several protective layers are placed on top of the sediments in order to isolate contaminants from the overlying water column. Traditional materials including sand, gravel and stone, as well as reactive barriers and less prevalent materials such as geotextiles and membranes can be used as filter material and erosion protection in the coverage (Zhang et al, 2016). Thus, this method can be designed in a variety of ways, with both inert and/or active materials, depending on the site-specific remediation needs and can therefore be suitable for both erosion- and sedimentation seabeds (Ramboll, 2019b). However, there are some drawbacks with this type of method as its required thickness, usually 20-50 cm (Olsen et al, 2019), makes it less suitable for shallow waters and also that the amount of material needed can be both expensive and time-consuming to apply depending on the size of the contaminated area (Ramboll, 2019b).

2.5 Thin-layer capping

A relatively new in-situ approach is the thin-layer capping technique, where an active material is placed on top of the sediment contributing to both containment and treatment of the contaminants (Zhang et al, 2016). This method has been recently implemented in projects in e.g., the USA and Norway and has gained increasing attention as the benefits include a reduced cost compared to other methods, suitability for both organic and inorganic pollutants, and the fact that it is less environmentally disruptive (Olsen et al, 2019). Furthermore, one benefit in comparison to the passive capping technique is the thickness of the cap. When adding active materials with sorption capacity, the amount of material as well as the thickness of the cover can be reduced, i.e., a thin-layer cap (Zhang et al, 2016). According to observations from large-scale field experiments in two fjord areas in Norway, a thin-layer cap can be as thin as 2.5-5 cm depending on the material chosen (Cornelissen et al, 2011; Cornelissen et al, 2012).

The objective of applying a thin-layer cap is to reduce contaminant mobility, toxicity and bioavailability. This is mainly generated by both sorption capacity of the material as well as reduced diffusion fluxes by increasing the diffusion path. In other words, the active material can change the phase of contaminants from aqueous to solid making them less bioavailable. Also, by increasing the K_d-coefficient (solid/liquid partition), the isolation period until contaminants break through the capping layer can be extended giving more time for natural deposition and degradation processes to occur (Zhang et al, 2016). However, some limitations exist when using the thin-layer capping method. With decreasing thickness of the capping layer, bioturbation and gas build up from the covered sediment are more likely to disrupt the capping material, allowing bound contaminants to re-enter the aquatic environment. It is therefore important to consider which material to use, as they have different properties, and how to implement the cap on a larger field-scale. Usually, several physicochemical tests are performed on the cover materials to be able to predict possible adsorption efficiencies and diffusion fluxes etc. for the contaminants indented to be immobilized and isolated.

2.5.1 Commonly used capping materials

Some of the most acclaimed active materials for removal of heavy metals and/or organic contaminants are zeolites, apatite minerals, organoclays, zerovalent iron and different carbonaceous materials (Knox et al, 2014; Yang et al, 2020). Zeolites, apatite minerals and organoclays have proven to decrease metal concentrations in the water column above the cap (Knox et al, 2014), and activated carbon (AC) has been shown to reduce levels of aqueous phase organic compounds, such as methyl-Hg, in benthic organisms (Zhang et al, 2016). Apatite minerals can be successfully used as a cap medium for heavy metal contaminated sediments. Due to its high cation exchange capacity, it can retain heavy metals and delay cap breakthrough but, on the other hand, it could also lead to additional contamination as apatite can contain high concentration of impurities such as As, Cr and U (Zhang et al, 2016). Other alternative materials are zeolites, used prevalently in e.g., water and wastewater treatment for removal of heavy metal and/or nutrients, and zerovalent iron, with an ability to reduce toxicity by immobilizing heavy metals and degrading organic contaminants (Wang & Peng, 2010; Zhang et al, 2016).

Active materials suited for, but not limited to, contamination of organic compounds are especially organoclays (organically engineered clays) and carbonaceous materials (Zhang et al, 2016). These are, like the other materials mentioned, considered as sorbents that change the geochemistry and increase contaminant binding. One of the most commonly used materials in active capping, nowadays, is activated carbon (AC) which is carbon processed from coal or biomass. It is usually applied either on top of the sediments on its own or mixed with other clean materials. The positive effects include reduced bioavailability and toxicity of the contaminants, but negative effects such as decreased efficiency of bottom fauna has been recognized (Olsen et al, 2019).

2.6 Biochar-based thin-layer capping

2.6.1 The fundamentals of biochar

Another carbonaceous material gaining interest in the active capping approach is biochar, which is a term more recently established to differentiate between activated carbon derived from coal and activated carbon derived from biomass (Joseph et al, 2015). Biochar can therefore perform similarly and have indistinguishable properties as other carbonaceous materials but is typically defined by its high level of organic carbon produced through pyrolysis of organic feedstock and by being designed for environmental management (Joseph et al, 2015; Zhang et al, 2016). Biochar can be carbon-neutral or even carbon-negative and has a high cation exchange capability and large specific surface area yielding a high adsorption capacity (Wang & Wang, 2019). To this day, biochar has been extensively proven to perform well in immobilizing heavy metals and organic pollutants in soil remediation and wastewater treatment, but research and implementation for contaminated sediments are limited (Yang et al, 2020; Wang et al, 2018). However, it can be considered highly suitable for sediment remediation as biochar outperforms other carbonaceous materials in terms of relative abundance and sorption abilities (Yang et al, 2020).

2.6.2 Biochar as an active capping material

Important parameters when using biochar as capping medium for remediating metal contaminated sediments heavily rely on biochar’s ability to: (1) sorb metals by e.g., electrostatic adsorption, complexation, ion exchange or precipitation (Thomas et al, 2020), (2) increase the pH and thus create an alkaline environment that retains the metal cations, and (3) contribute to a carbon-rich environment that enhances microbial activities and changes the redox conditions (Wang et al, 2018). Thus, how well biochar performs depends on physical and chemical characteristics such as pore structure, pH, surface charge and functional groups which can differ depending on type of feedstock and pyrolysis temperature (Thomas et al, 2020; Yang et al, 2020). A biochar with a higher ash content, for example, results in higher pH that increases metal retention (Wang et al, 2018). From a review carried out by Thomas et al (2020) where data was analyzed from several publications on biochar’s performance as a soil amendment it was prominent that biochar's sorption potential and ability to attract metals increases with a nutrient-rich feedstock and high aromaticity (i.e., high O/C ratio). Furthermore, it was also observed that biochar exhibits a higher adsorption capacity for Pb(II) and Cd(II) than for Zn(II) and As(V).

The biochar approach for sediment remediation has been studied for carbon sequestration and sorption of heavy metals, such as Cu(II), Pb(II), Cd(II), Zn(II) and Hg(II) (Ghosh et al, 2011, Yang et al, 2020; Zhang et al, 2016). However, biochar performs better when the functional groups of biochar, such as -COOH, -OH, $-NH_4^+$ etc., can interact with sediment contaminants and therefore immobilize them (Yang et al, 2020). One drawback to consider in application of biochar as a thin-layer cap is the changes in habitat for benthic organisms. Observations in one of the field-tests in Norway showed that the 2-5 cm thick AC layer had been mixed into the sediment by 3-4 cm after 12 months (Cornelissen et al, 2011). Furthermore, Yang et al (2020) states that further research of biochar toxicity on aquatic organisms is needed, but it is evident that benthic organisms can cause biochar particles and contaminants to enter the water body by feeding and digging into the capping material.

2.6.3 Materials to aid deposition of biochar

When using biochar for the application of a thin-layer cap, the settling property of biochar is an important consideration due its low density, with typical values of 90-500 $kg \cdot m^{-3}$ depending on type of feedstock (Joseph et al, 2015). To aid the deposition of biochar, it can be beneficially used together with another active and/or conventional material (Yang et al, 2020). Which material to use, depends on the objective and characteristics of the site. A site with high-flow water requires a more stabilizing material while at a more closed off site, the main focus in choosing material can be to aid the retention of contaminants. For example, sand and gravel-based materials can be successfully applied for deposition of biochar while a clay-based material also can increase the adsorption of contaminants (Naturvårdsverket, 2003). In a field experiment in the Trondheim harbour in Norway, a thin-layer cap using AC mixed with bentonite clay for PAH-contaminated sediment showed decreased PAH fluxes, higher AC recoveries (60% vs 30%) and less adverse effects on benthic organisms in comparison to AC mixed with sand (Cornelissen et al, 2011). However, sand can still be an option for covering an AC/biochar layer and protect against erosion. It is important to consider the objective of the remediation and also factors of the materials, such as their cost, chemical stability and environmental footprint (Olsen et al, 2019; Yang et al, 2020).

3 Method and materials

3.1 Sampling site and sediment collection

The sediment in the Bureå bay was collected in November 2020 using a Van Veen grabber at coordinates 64°37'24.5"N, 21°14'20.5"E. The sample site is located slightly northeast of the previous active industry property and marked as “test area” in Figure 2. Water depth at the sampling site was about 2 m and samples were taken from the upper 20-30 cm of the sediment. The area was divided into a 30x30 m grid where sediment was collected from 9 locations (3, 4, 5, 9, 10, 11, 15, 16, and 17) and placed as composite samples in plastic buckets of 15 liters to be sealed and stored in a storeroom at ambient temperature. One of the sample buckets was homogenized in the laboratory to be used for the column experiment set up. Larger debris was removed using a sieve of 1 cm. Photos of the sediment are shown in Appendix A.

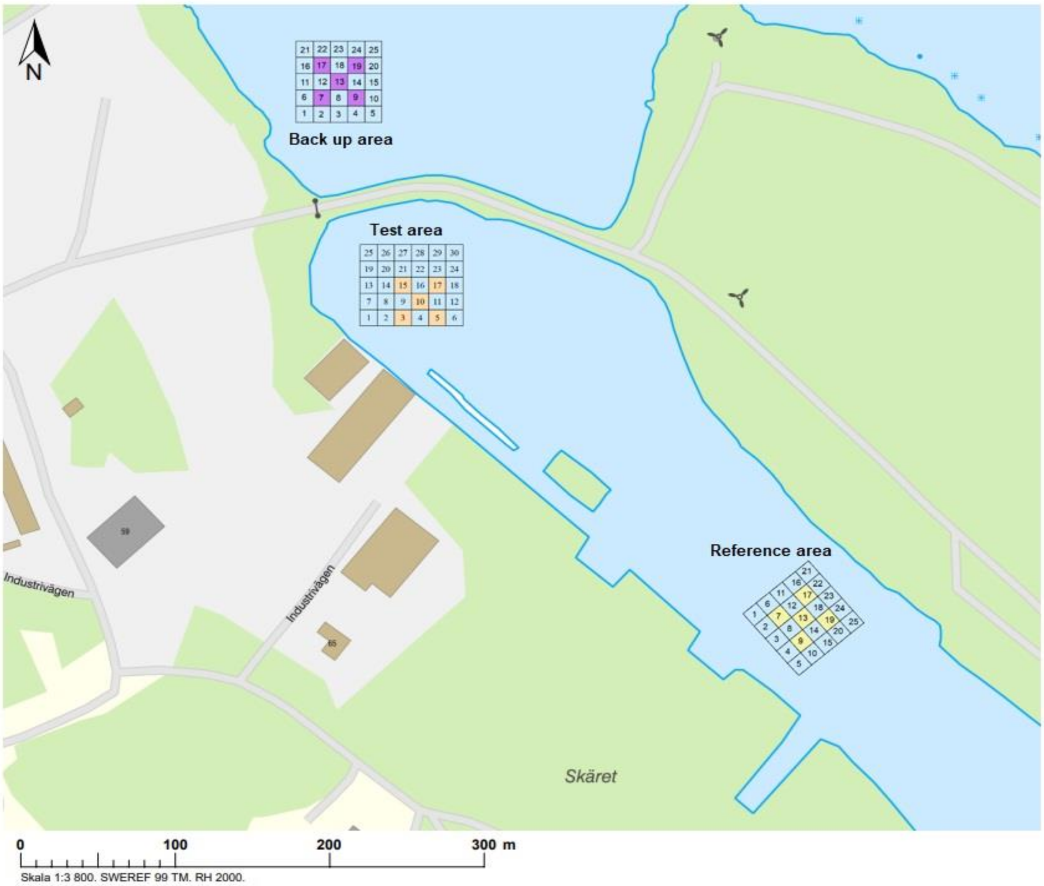

Fig 2. The Bureå site, showing the sampling grid of the test, back up and reference area. Sediment used in this study is sampled from the test area.

Seawater for the column experiment was sampled in 3x20 L plastic containers at Lövskär sea area in the vicinity of Luleå in January of 2021. Seawater at this site was assumed to have similar composition as that in the Bureå sea area and was collected due to accessibility. The EC and pH were measured in the field at the Lövskär site and one 60 mL sample was collected for metal analysis. Later in the spring in March 2021, EC and pH in the overlying water column at Burefjärden were determined by in situ measurements at water depths of 1 and 2 m with a pH/cond-meter (Mettler Toledo SevenGo Dou SG23). Water samples for determination of oxygen saturation were collected in 2x110 mL glass bottles at each depth and sent to ALS Scandinavia AB in Luleå for analysis.

3.2 Capping materials

Biochar was used in all test-caps, combined with the structural materials bentonite clay, rock dust of two different particle sizes, and a concrete slurry. The first materials chosen for the tests were biochar and bentonite, as biochar (powdered AC) mixed with bentonite clay have been previously shown to perform well in marine environments (Cornelissen et al, 2011). Furthermore, these are the materials that will be used in the pilot-scale project at the Bureå site in spring of 2021. Two different rock dusts and a concrete slurry were then chosen to be evaluated for their suitability to replace the expensive bentonite as a structural material to aid in deposition of biochar. These materials are excess materials from different industrial sites and were chosen for their availability as they could be collected at sites near Luleå.

The biochar was acquired by Jacobi Carbon AB (Kalmar, Sweden) and is of type CP1 with an active area of 1050 $m^2 \cdot g^{-1}$ made from coconut shell-based material. Note that this product is promoted as an activated carbon, but in this study the term biochar is used due to it being refined and produced from plant-based organic feedstock. The bentonite clay is a dry powdered white sodium montmorillonite, saline seal from CETCO and was obtained from FLA Geoprodukter (Luleå). A test of the swelling capacity of bentonite was performed prior to the column experiment resulting in a 50 g of bentonite yielding an approximately 4 cm thick layer in the experimental columns. In the columns, 2 g of NaCl was added (4 % of the bentonite weight) to reduce the swelling and reach the desired thickness of the cap. Rock dust of grain size 0-2 mm (water content 1.3 %; LOI 0.09 %) and 0-0.5 mm (water content 16.0 %; LOI 0.14 %) was collected from Rutviks quarry (Swerock AB) and Peab Asfalt in Boden, respectively. The concrete slurry (water content 65.7 %, LOI 0.98 %) was acquired from Swerock AB in Boden and is excess concrete from concrete trucks mixed with water. Photos of the capping materials are shown in Figure 3.

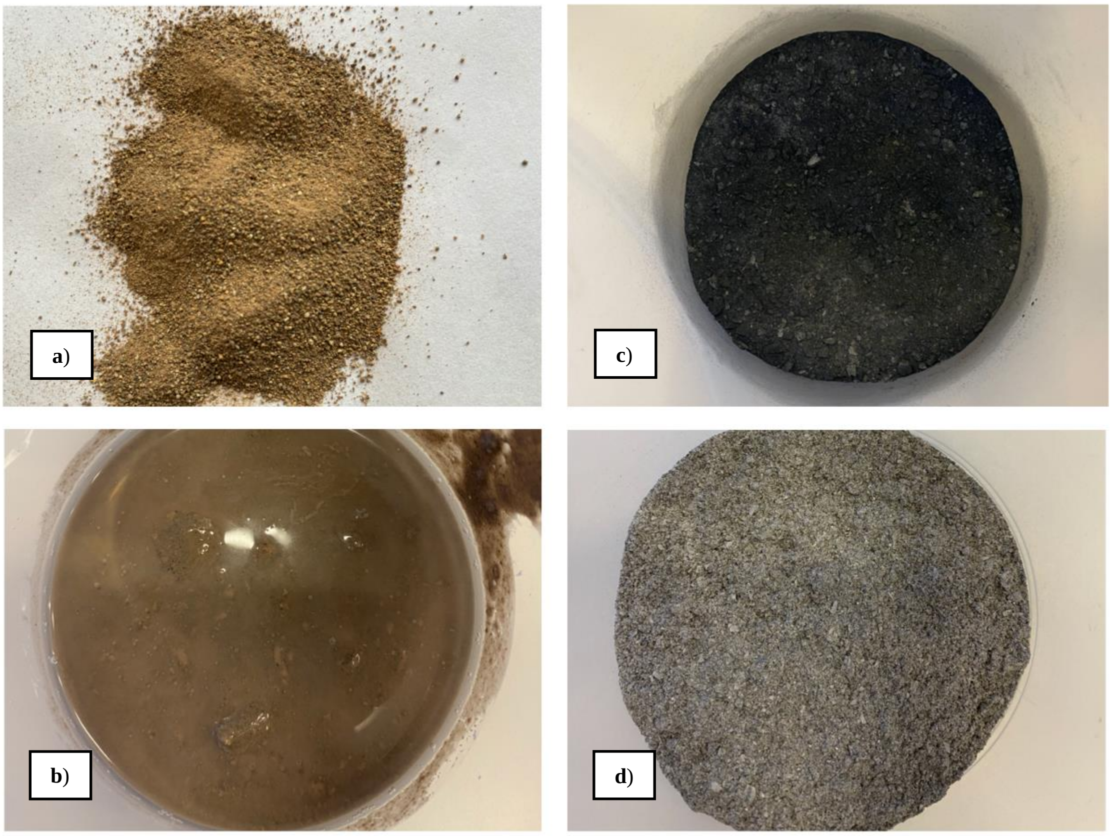

Fig 3. Capping materials acquired to aid in biochar deposition where **a)** shows powdered bentonite clay, **b)** concrete slurry, **c)** rock dust of 0-0.5 mm (rd005) and **d)** is rock dust of 0-2 mm (rd02).

3.3 Bench-scale capping experiment

The performance and efficiency of the various capping materials was evaluated by a bench-scale laboratory set up with triplicates of each test. Four experimental set ups were performed: (1) no capping for sediment control, (2) only capping material for material control, (3) sediment mixed with biochar and (4) sediment capped with each material mixed with biochar (Figure 4). A total of 18 glass columns, 10 cm in diameter and 30 cm high (Figure 5a), and 8 plastic containers, 10x10 cm in size, were used for the set up. The plastic containers were used for control of substance release from each material and the glass columns for evaluating the capping efficiencies. Approximately 6 cm of marine sediment (60.1 ± 4.4 $\text{kg}\cdot\text{m}^{-2}$ (n=18)) was added in all the columns. In the first three columns the sediment was left uncapped. Biochar (0.8 $\text{kg}\cdot\text{m}^{-2}$) was mixed into sediment in the three next columns and mixed into pastes of bentonite (2 $\text{kg}\cdot\text{m}^{-2}$), rock dust (20 $\text{kg}\cdot\text{m}^{-2}$) and concrete slurry (20 $\text{kg}\cdot\text{m}^{-2}$), also in triplicates, in the remaining 12 columns. The pastes were placed on top of the sediment layer with a cap thickness of approximately 2-4 cm. The proportions between capping materials and seawater were chosen so that enough water was available in the columns for extraction during three sampling occasions (Figure 4). For material control, duplicates of each material were placed in the plastic containers with de-ionized MilliQ water on top. To evaluate the bentonite clay's adsorption capacity without the biochar, the bentonite clay was placed on top of a sediment layer with added seawater on top in two of the plastic containers. Three times during the 8-week test period, 60 mL of the overlying water in the glass columns was extracted at 10 cm depth using plastic syringes and tubes (Figure 5c). The extracted samples were filtered (0.45 µm) into plastic bottles (Figure 5d). Control samples with de-ionized MilliQ water were collected after 60 days to identify any trace elements concentrations released by the materials.

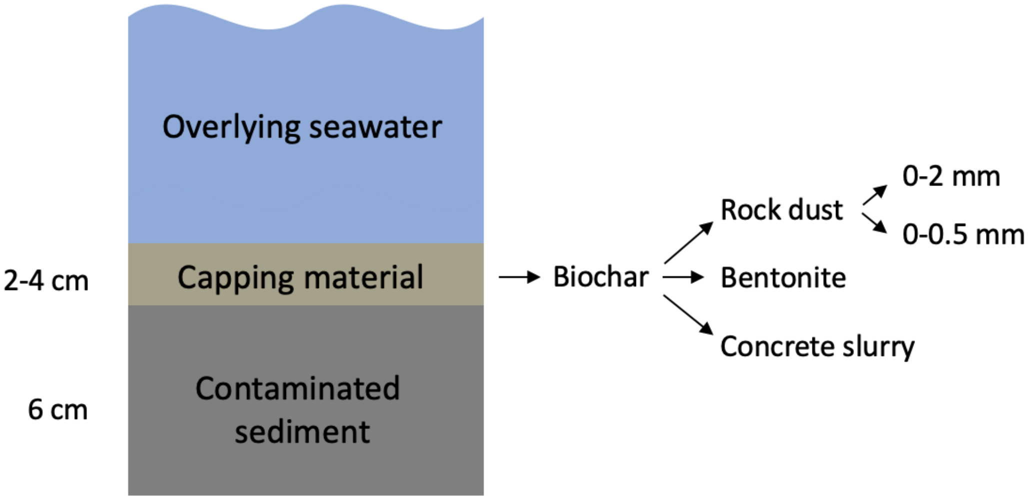

Fig 4. Picture illustrating the proportions of the different layers in the experimental columns. The experiment was performed with triplicates of uncapped sediment, triplicates of sediment mixed with biochar and triplicates of each of the biochar and material mixtures.

Fig 5. The experimental set up: where **a)** displays the 6 cm sediment layer and **b)** sediment with addition of the 2-4 cm thick capping layers and water column on top. Pictures **c)** and **d)** shows syringe, tube and filter used for water extraction at the three sampling occasions.

3.4 Analytical methods

Collected samples of sediment and sediment pore water, capping materials, extracted water from the columns, and Bothnian Bay water from Bureå and Lövskär were all sent to ALS Scandinavia AB in Luleå and analyzed according to Swedish Standard methods. Concentrations of metals in sediment and capping materials were determined after digesting the samples in 7M HNO_3 in a hotblock. Metal concentrations were then determined by Inductively Coupled Plasma-Sector Field Mass Spectrometry (ICP-SFMS), Inductively Coupled Plasma Atomic Emission Spectroscopy (ICP-AES) and Atomic Fluorescence Spectroscopy (AFS). Dry weight (TS) of the Bureå sediment and the capping materials were determined by the TS-105 method. For analysis of sediment-to-water transportation of trace elements, 60 mL of seawater in each column was extracted on three sampling occasions after 19, 33 and 60 days, and sent to ALS Scandinavia AB where metal concentrations were determined by ICP-SFMS, ICP-AES and AFS. Chloride and sulfur were determined by ion chromatography. All the samples were acidified by 1 ml HNO_3 per 100 ml before analysis. The pH and EC were measured in the columns using a Mettler Toledo SevenGo Dou SG23 pH/Cond-meter. The methods of analysis and the included elements and/or parameters are compiled in Table 2.

Table 2. Description of methods used to determine the sediment, capping material, water and pore water concentrations at ALS Scandinavia AB in Luleå.

Analysis	**Method**	**Included elements/parameters**
Metals in fresh water	ICP-AES (W-AES-1A) and ICP-SFMS (W-SFMS-5A) according to SS-EN ISO 11885:2009 and SS-EN ISO 19729-2:2016. Hg determined by AFS (W-AFS-17V2) according to SS-EN ISO 17852:2008. The samples were acidified with 1 ml HNO_3 (suprapur) per 100 ml before analysis.	Ca, K, Mg, Na, Si, Sr, Al, As, Ba, Cd, Co, Cu, Hg, Fe, Mn, Mo, Ni, P, Pb, V, Zn
Chloride and sulfate in fresh water	Determined by ion chromatography according to CSN EN ISO 10304-1 and CSN EN 16192.	Cl, SO_4
Salinity and dissolved O_2 in fresh water	Salinity determined by electrical conductivity by conductometer and calculation of salinity according to CSN EN 2788, SM 2520 B and CSN EN 16192. Oxygen determined by electrochemical method according to EN 25814.	Salinity, O_2
Metals in pore water	Determined by ICP-AES (W-AES-1B) and ICP-SFMS (W-SFMS-5D) according to SS-EN ISO 11885:2009 and SS-EN ISO 19729-2:2016. Hg determined by AFS (W-AFS-17V3a) according to SS-EN ISO 17852:2008. The samples were acidified with 1 ml HNO_3 (suprapur) per 100 ml before analysis.	Ca, K, Mg, Na, Si, Sr, Al, As, Ba, Cd, Co, Cu, Hg, Fe, Mn, Mo, Ni, P, Pb, V, Zn
Metals in soil, sludge, sediment and construction material	Analyzed by ICP-SFMS (S-SFMS-59) according to SS-EN ISO 17294-2:2016 after digestion in 7M HNO_3 in hotblock (S-PM59-HB) according to SE-SOP-0021.	As, Ba, Cd, Co, Cr, Cu, Hg, Ni, Pb, V, Zn
Dry weight of soil, sludge, sediment and construction material	Determination of dry weight (TS-105) according to SS-EN 15934:2021 utg 1.	TS at 105 °C

4 Results and Discussion

4.1 Water profile in Burefjärden

Results from in-situ measurements of temperature, pH, and conductivity (EC) in the water profile are presented in Table 3. The pH at the site is marginally acidic and shows a minor decrease with depth (6.3 to 6.2). A significant increase in conductivity can be observed with depth, approximately 8 times higher at 2 m, indicating a shallow and poorly mixed water. As salinity controls conductivity, the salinity at the site is assumed to increase considerably with depth as well and is estimated to ≤2 ppt. Measurements were performed in March when the bay was ice covered and thus, to make a more reliable assessment of the waters' physicochemical profile, complementary sampling throughout all seasons would be necessary. Seasonal changes in temperature, salinity and primary production may cause variations in redox and pH conditions at the site. However, these measurements can be used as an indication of the physicochemical conditions in order to correlate the assessment of trace element behavior in the experimental columns to in situ conditions. For instance, the relatively low pH at the site could indicate that contaminants are more likely to be released from the sediment and further sustaining the polluted conditions.

As stated previously, distribution and partitioning of metals in sediment are mainly regulated by redox and pH conditions. The water profile at the site is assumed to be oxygenated due to continuous inflow of river water and the low bioproduction in the Bothnian Bay. VISS (2020) have published data from an oxygen condition monitoring program during 2008-2013, which shows that the oxygen conditions in the Burefjärden sea area are classified as "high" ($>5\ mg \cdot L^{-1}$) according to HVMFS 2019:25. However, conditions deeper down near the sediment surface are assumed to be suboxic to anoxic due to the fiber rich residues in the sediment. The seawater added in the laboratory columns was sampled at Lövskär harbor, about 150 km from the Burefjärden sea area, and is assumed to have similar levels of dissolved O_2 as the seawater at the site. However, levels of dissolved As and Hg, along with other trace elements, are likely lower in the Lövskär seawater than in Bureå bay due to contributions from the Skellefte Sulfide Ore District and the Rönnskärsverken smelter at Skelleftehamn (Figure 1).

Table 3. In-situ measurement of temperature, pH and EC at two depths in Burefjärden sea area.

Depth (m)	Temp (°C)	pH	EC ($\mu S \cdot cm^{-1}$)
1	2.2	6.3	236
2	2.4	6.2	1976

4.2 Properties of the sediment and capping materials

Samples of sediment and capping materials were sent for analysis before experimental set up. Results are presented in Table 4, where concentrations in sediment and capping materials (in mg·kg^{-1} dry weight) are compared with available guide values (class V "very high content") from Naturvårdsverket's assessment criteria for metals in marine sediment (Naturvårdsverket, 1999). Though they are not technically a sediment, the capping materials are also compared to these values in this study as they are intended to be distributed in a marine sediment. Complete analysis protocol is available in Appendix B.

Table 4. Metal concentrations in sediment and capping materials. Classification "very high content" represents class V of heavy metal contamination levels (mg·kg^{-1} dry weight) for assessment of metals in marine sediment according to standard Swedish method (Naturvårdsverket, 1999). Levels exceeding class V in *cursive*.

Material	As	Cd	Cr	Cu	Hg	Ni	Pb	Zn
Unit	mg·kg^{-1}	mg·kg^{-1}	mg·kg^{-1}	mg·kg^{-1}	mg·kg^{-1}	mg·kg^{-1}	mg·kg^{-1}	mg·kg^{-1}
Class V	**>45**	**>3**	**>72**	**>80**	**>1**	**>99**	**>110**	**>357**
Sediment	*240*	*4*	42	*93*	*2*	17	*196*	183
Rockdust02	6	<0.1	57	66	<0.2	33	12	90
Rockdust005	0.7	<0.1	33	13	<0.2	8	3	89
Concrete slurry	4	0.3	26	36	<0.2	14	12	*468*

The marine sediment sampled in Burefjärden displays elevated levels of As (240 mg·kg^{-1}), Pb (196 mg·kg^{-1}), Cu (93.3 mg·kg^{-1}), Cd (4.11 mg·kg^{-1}) and Hg (1.66 mg·kg^{-1}). These levels represent the test area which displays lower concentrations than the average levels from 34 sampling points around the area (Table 1 in section 2.1.1). This study was performed by Ramboll (2019a) and indicates that the contamination is not evenly distributed at the site, and "hot spots" may occur. Earlier sampling campaigns in the area displayed significantly higher Hg and As levels, as maximum concentrations were about 11 times higher (18 mg·kg^{-1} for Hg and 2460 mg·kg^{-1} for As) than the measured concentrations at the test area. Thus, results obtained from the experimental set up using this sediment may not be representative for the whole of the area, but only give indications of the efficiency of the different thin-layer caps. As presented in Table 4, the larger-grained rock dust displays higher levels of heavy metals than the finger-grained. Dissolved metal concentrations are generally low, with exceptions; rockdust02 exhibiting slight to high risk for Cu content, and the concrete sludge displaying elevated levels of Zn (468 mg·kg^{-1}) that exceeds classification V.

4.2.1 Application of capping materials

Difficulties when applying the capping layers were observed during the laboratory experiment. The two rock dust materials were technically easy to apply in the controlled laboratory environment but would most likely be challenging on a larger field-scale. The finer grained rock dust, with its small particle size and low moisture content (0.2 %), displayed some difficulties settling and was therefore not particularly successful at aiding the deposition of biochar. The same difficulties were observed for the larger-grained rock dust (Figure 6c), where a clearly visible layer of biochar can be noted on top of the capping layer and at the water column surface. Note that these two materials, due to technical challenges, were mixed with biochar and added as dry powders on top of the sediment layer. These dry layers were slurried when adding seawater on top making the rock dust materials settle faster than the biochar, resulting in the layering of the materials seen in Figure 6. Concrete sludge and bentonite clay were added as pastes and showed similar layering characteristics when applying them. However, it can be observed in Figure 6 that the biochar+bentonite layer yielded a thicker, more uneven cap due to its swelling capacity. Furthermore, the biochar+concrete slurry paste did not exhibit any visible layering of biochar. The loss of biochar is insignificant in the controlled laboratory environment and could therefore not be taken into further consideration in this study. Nevertheless, it is viable to assume that the rock dust materials would result in a greater loss of biochar, than the bentonite and concrete slurry pastes, due to the visible layering and the biochar film on top of the water column.

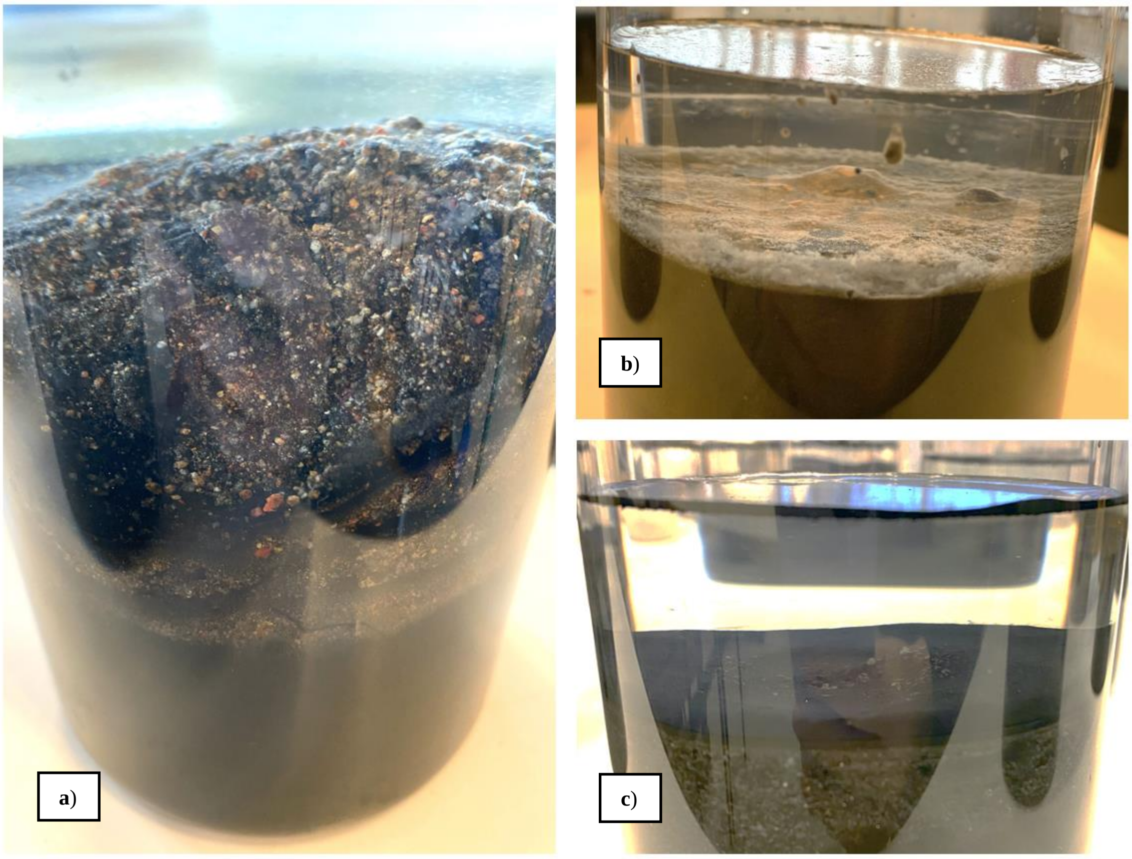

Fig 6. a) biochar+bentonite capping layer after 60 days, **b)** biochar+concrete slurry with no visible biochar layering and **c)** biochar+rock dust (0-2 mm) where a thin biochar layer is clearly visible.

4.3 Conductivity and pH in the overlying water column

This section summarizes the measured pH and conductivity conditions in the laboratory column set up. Changes in pH are presented in Figure 7, and conductivity in Figure 8. Both the pH and conductivity were measured over the course of 60 days, and the graphs display calculated averages for measured values in the triplicate columns for each capping material. Standard deviation (SD) was calculated for each pH value and showed good precision, with a maximum observed SD of ±4% for the biochar+bentonite column. All measured pH and conductivity values are available in Appendix C.

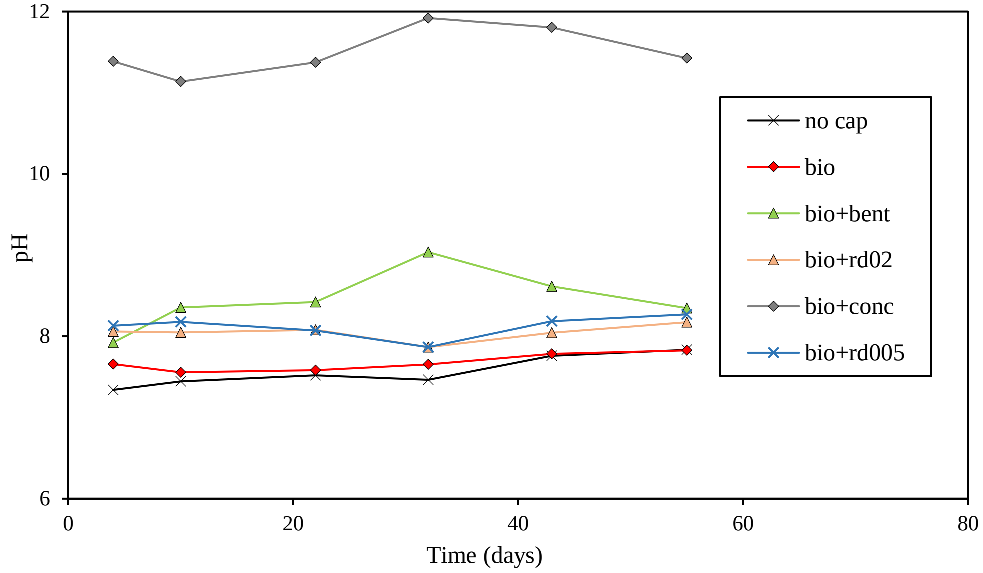

Fig 7. Average pH in the seawater measured at approximately 10 cm above uncapped and capped sediment layers at six occasions during the course of 60 days.

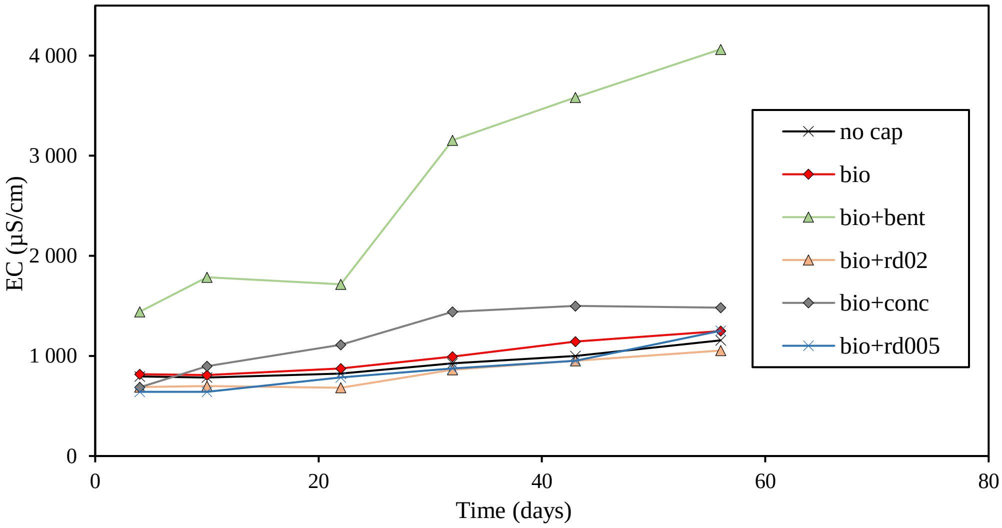

Fig 8. Average conductivity (µS·cm^{-1}) in the seawater measured at approximately 10 cm above uncapped and capped sediment layers at six occasions during the course of 60 days.

Initial pH in the seawater was measured to neutral (7.0) and an increase in pH can be observed in all columns (Figure 7). The uncapped sediment increases pH in the seawater slightly (7.6) followed by biochar <biochar+rockdust02 <biochar+rockdust005 <biochar+bentonite <biochar+concrete slurry. A small increase in pH (7.7) was observed when biochar was mixed into the sediment. This indicates that the application of biochar, which is an alkaline material, increases the pH in the columns. Addition of biochar+rockdust increases pH to >8 and biochar+bentonite clay to an average pH of 8.5. A significant increase in pH can be observed in the biochar+concrete slurry columns (11.5), which likely responds to the limestone binder in the concrete. An indication of this was an observed average release of 692 mg·L^{-1} of Ca in the columns.

The conductivity in the columns is generally increasing with time as ions are released into the overlying seawater (Figure 8). The increase in conductivity indicates that dissolved substances are released from the sediment and/or capping layers over time. The average conductivity for all of the columns increases from about 600-800 µS·cm^{-1} to 1000-1400 µS·cm^{-1} during the 60-day period, except for biochar+bentonite which exhibits a significantly higher conductivity due to added NaCl for reducing the layer thickness. World average sea water has a conductivity of about 50 000 µS·cm^{-1} (salinity 35 PSU) according to MRCCC (n.d.) (salinity 35 PSU). The Bothnian Bay is, however, a brackish water more similar to freshwater composition, which according to MRCCC (n.d.) usually exhibits a conductivity in the range of 0-1500 µS·cm^{-1} (salinity 2-4 PSU).

4.4 Sediment-to-water release of trace elements

Concentrations of trace elements were analyzed from samples extracted in the seawater at about 10 cm depth in the columns after 19, 33 and 60 days. Where available, assessment criteria for special pollutants in coastal waters will be used to determine possible toxic effects of the metals. These criteria are based on ecological assessments and bioavailability of the elements and have been developed by Swedish Agency for Marine and Water Management (HVFMS 2019:25).

Average concentrations were calculated from measurements in the triplicate columns for each material. The average concentrations (µg·L^{-1}) and SD above each capping layer after 60 days for As, Cd, Cu, Hg, Pb and Zn are presented in Figure 9. Figure 10 shows average concentrations and SD above each capping layer after 60 days for Al, Fe, Mn and P. Full analysis results from the column experiment are available in Appendix B. Average concentrations for the control samples of the materials are presented in Table 5. Selected trace element concentrations over time are discussed in following sections below.

Table 5. Average concentrations in water column (de-ionized MilliQ) above the capping materials in duplicate plastic containers after 60 days. Note that bentonite clay control is with sediment layer and seawater.

Material	As	Cd	Cr	Cu	Hg	P	Pb	Zn	Al
Unit	µg·L^{-1}	µg·L^{-1}	µg·L^{-1}	µg·L^{-1}	µg·L^{-1}	µg·L^{-1}	µg·L^{-1}	µg·L^{-1}	µg·L^{-1}
Bentonite[1]	436	0.006	0.177	4	<0.002	1443	0.1	9	3
Rockdust02	2	0.006	0.04	0.6	<0.002	5	0.1	2	153
Rockdust005	12	0.03	0.2	5	<0.002	170	0.02	1	43
Concrete slurry	0.3	0.003	4	3	<0.002	3	3	7	135

[1] Bentonite control sample=only bentonite capping layer (no biochar) above sed layer.

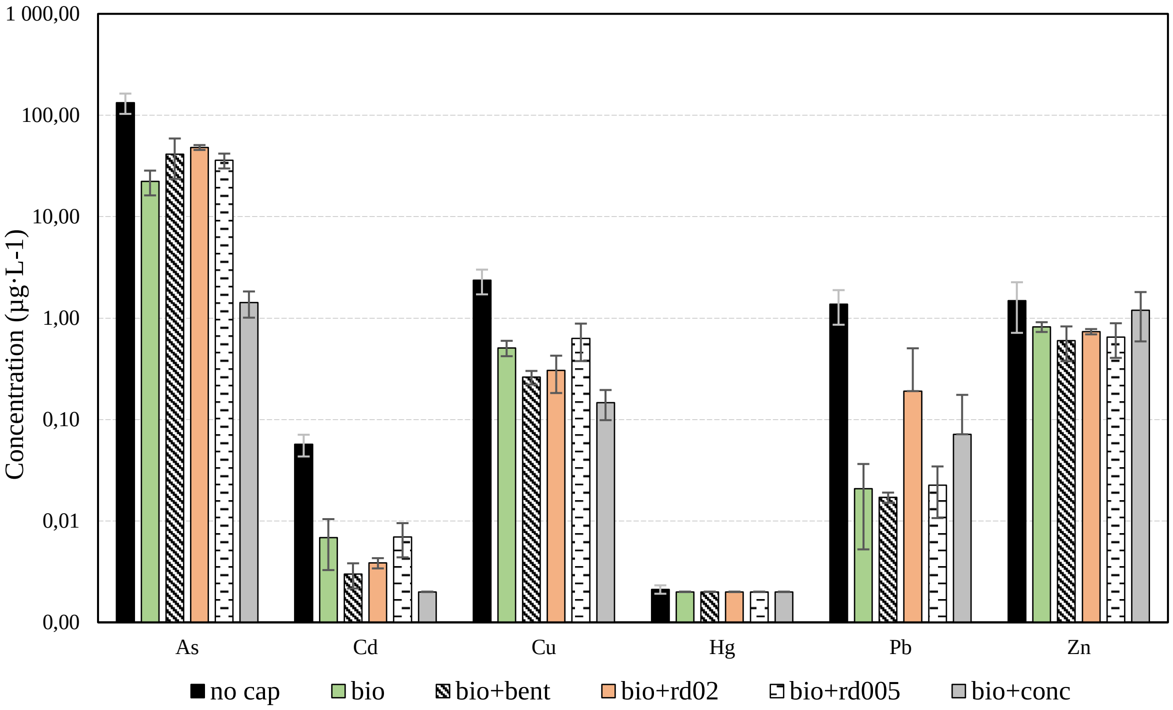

Fig 9. Average concentrations (µg·L^{-1}) of As, Cd, Cu, Hg, Pb and Zn above the sediment with no capping and different capping materials in the columns after 60 days. Error bars show calculated SD. Cd was below detection limit (<0.002 µg·L-1) in the concrete columns and Hg in all columns except for the uncapped sediment.

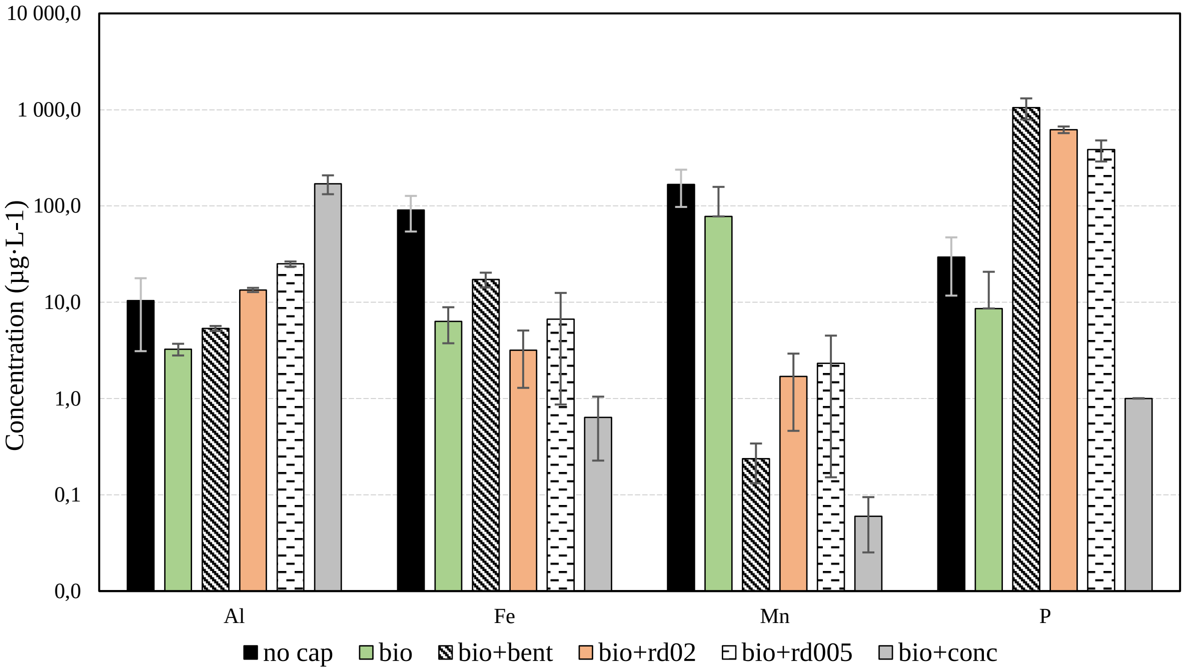

Fig 10. Average concentrations (µg·L^{-1}) of Al, Fe, Mn and P above the sediment with no capping and different capping materials in the columns after 60 days. Error bars show calculated SD.

In Figure 9 it can be observed that all capping materials prevent and/or delay release of heavy metals after 60 days. Mercury levels were below detection limit in the columns, indicating that either methylation of Hg (Me-Hg) has occurred or anoxic conditions in sediment that favors formation of insoluble Hg-sulfides. Furthermore, Pb and Cd are the elements displaying the largest decrease in concentrations in the biochar columns compared to other elements. This agrees with earlier findings presented by Tomas et al (2020) where biochar showed a higher adsorption capacity for Pb and Cd than Zn and As (V).

Average levels of As can be observed as significantly higher than the other elements in all columns. The black bars (no cap) in Figure 9 represents the average concentration in the water above the uncapped sediment which displays the highest levels for all elements after 60 days. However, the thin-layer capping materials delay release of As which can be noted by a reduction of the As level above the uncapped sediment (133 ± 30 $\mu g \cdot L^{-1}$) by a factor of 3 in the biochar+rock dust02 columns, and by a factor 95 in the biochar+concrete slurry columns.

Figure 10 shows that release of Fe and Mn is prevented by the capping materials while levels of dissolved Al and P are increasing in most of the columns. In the biochar columns, the levels are decreasing which might indicate a higher adsorption efficiency when biochar is mixed into the sediment. Furthermore, results of the material control in Table 5 show that 1443 ± 176 $\mu g \cdot L^{-1}$ of P is released with only bentonite as a capping material. For Al, increasing dissolved levels for rock dust of larger grain size (153 $\mu g \cdot L^{-1}$) and concrete slurry material (135 $\mu g \cdot L^{-1}$) are likely to stem from the added materials, and less likely to have been transported from sediment through the capping layers.

To summarize, the compiled concentrations in Figure 9 and Figure 10 show that all the thin-layer caps generally prevent release of metals and P, and the probable main cause would be a reduced diffusion through the added layers and/or the adsorption capacity of the biochar. Furthermore, the capping layers exhibiting increasing pH values also displays lower levels of dissolved heavy metals after 60 days.

4.4.1 Iron, manganese and sulfate

In order to gain knowledge of the redox conditions in the columns, the partitioning and distribution of redox sensitive elements, e.g., Fe, Mn and S, can be evaluated. Iron and Mn form hydroxides and oxides at oxidized conditions resulting in decreasing dissolved Fe and Mn concentrations. This can occur both in the water column and in the sediment pore water, and other trace elements are usually sorbed to the Fe and Mn hydroxides. These hydroxides are not stable in suboxic-anoxic conditions, when they dissolve easily yielding a mobilization of Fe, Mn and trace elements in the columns. Average concentrations of sulfate, iron and manganese after 19, 33 and 60 days in the water column above the different capping layers are presented in Table 6. In Figure 11, the average concentrations of Fe and Mn are presented in a bar diagram. The black bars represent average Fe concentrations, and the blue bars show Mn levels.

Table 6. Average concentrations of SO_4 (mg·L^{-1}), Fe (µg·L^{-1}) and Mn (µg·L^{-1}) over time in the water column at 10 cm above the sediment and capping layers. Samples were collected after 19, 33 and 60 days. Standard deviations (SD) were calculated for the triplicate columns at each sampling occasion.

	SO4-19	**SO4-33**	**SO4-60**	**SD-19**	**SD-33**	**SD-60**
no cap	23	23	35	2	3	12
bio	28	31	46	2	2	1
bio+bent	49	71	79	6	1	5
bio+rd02	20	22	23	0	2	1
bio+rd005	25	27	29	0	3	1
bio+conc	8	7	5	1	1	0
	Fe-19	**Fe-33**	**Fe-60**	**SD-19**	**SD-33**	**SD-60**
no cap	449	480	91	158	178	37
bio	68	57	6	2	5	3
bio+bent	66	44	17	6	4	3
bio+rd02	65	58	3	5	5	2
bio+rd005	85	60	7	9	17	6
bio+conc	1	1	1	0,5	0,4	0,4
	Mn-19	**Mn-33**	**Mn-60**	**SD-19**	**SD-33**	**SD-60**
no cap	274	313	168	69	79	70
bio	149	186	78	20	27	80
bio+bent	2	1	0,2	0,2	0,4	0,1
bio+rd02	1	1	2	1	0,4	1
bio+rd005	9	13	2	3	4	2
bio+conc	0,03	0,03	0,06	0,00	0,00	0,03

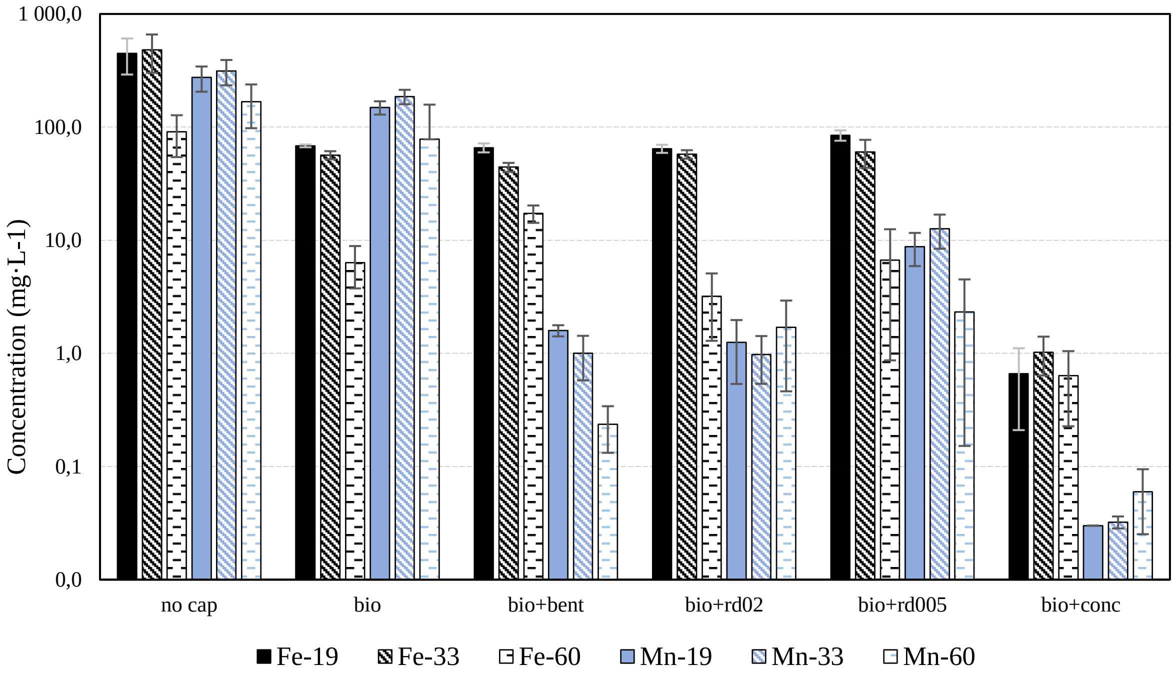

Fig 11. Average concentrations (µg·L^{-1}) for Fe and Mn over time in the water column above the uncapped and capped sediment in the experimental columns. The samples were collected after 19, 33 and 60 days. Error bars show calculated SD.

Overall, iron and manganese levels follow the same trend. In Table 6 it can be observed that Fe is reduced from 449 ± 158 $\mu g \cdot L^{-1}$ in the uncapped column to approximately 91 ± 37 $\mu g \cdot L^{-1}$ after 60 days. Mn is reduced from 274 ± 69 $\mu g \cdot L^{-1}$ to 168 ± 70 $\mu g \cdot L^{-1}$ in the same time frame. After 60 days, the different capping materials displays Fe concentrations in the low range of 0.6 to 17 $\mu g \cdot L^{-1}$. Biochar+concrete layer shows the lowest dissolved Fe level and biochar+bentonite the highest of the materials. The biochar+concrete layer displays the lowest Mn levels as well, of approximately 0.06 $\mu g \cdot L^{-1}$, while the highest levels can be observed in the biochar columns (78 $\mu g \cdot L^{-1}$) after 60 days. In general, the concrete slurry is most efficient at immobilizing Fe and Mn (Figure 11) which is the material yielding the most significant pH increase. This could indicate that the capping material and the upper part of the sediment is relatively oxidized, as Fe and Mn are more likely to form easily soluble hydroxides under oxidized conditions at neutral to mildly acidic conditions.

For the columns exhibiting a lower pH, more Fe, Mn and SO_4 can be mobilized and released through the capping layers. Additionally, levels of dissolved SO_4 are also significantly lower (5 $mg \cdot L^{-1}$, Table 6) in the capping layer with pH 11.5, which might suggest that reducing conditions are still prevalent in the sediment as Fe and Mn can be bound as sulfides. The release of Fe, Mn and SO_4 presented in Table 6 strengthens the conclusion that the sediment is reduced but with an oxidized surface yielding an upward migration of Mn, Fe, As and P. Furthermore, the trace elements are more likely to sorb/co-precipitate at the sediment-capping layer interface when adding a capping material that increases the pH in the sediment surface.

4.4.2 Copper and zinc

Average concentrations of Cu and Zn after 19, 33 and 60 days in the water column above the different capping layers are compiled in Figure 12. The black bars represent Cu concentrations, and the orange bars show Zn levels.

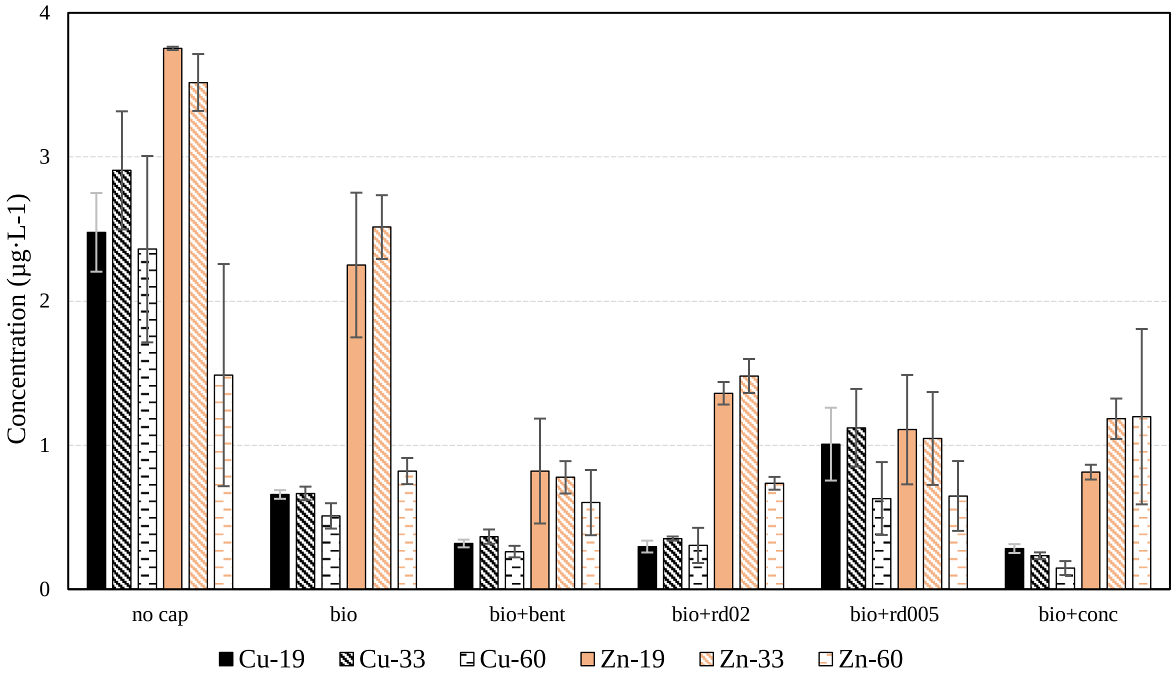

Fig 12. Average concentrations (µg·L^{-1}) for Cu and Zn over time in the water column above the uncapped and capped sediment in the column experiment. The samples were collected after 19, 33 and 60 days. Error bars show calculated SD.

In Figure 12 it can be observed that the level of dissolved Cu follows the same trend over time for all columns. Cu levels generally increase between 19 and 33 days, and then decrease at 60 days. It is only the biochar+concrete layer that shows continuously decreasing Cu levels over time. The highest displayed levels for all sampling occasions are in the water column above the uncapped sediment with Cu levels that ranges from 2.4 to 2.9 µg·L^{-1}. This can be compared to a maximum allowed Cu concentration in the Baltic Sea of 0.87 µg·L^{-1} according to HVFMS 2019:25. The bentonite clay (0.3 ± 0.04 µg·L^{-1}), rock dust of larger grain size (0.3 ± 0.1 µg·L^{-1}) and the concrete slurry (0.2 ± 0.1 µg·L^{-1}) show the highest efficiency for preventing release of Cu in a time frame of 60 days and is below the criteria level for Cu. However, considering the SD shown by the error bars, there variations in Cu concentration are not statistically significant.

Zn exhibits trends similar to Cu, with concentrations remaining approximately constant up to day 33, and then decreasing after 60 days for all capping layers except biochar+concrete material which increasese with time (Figure 12). However, considering the SD shown by the error bars, these variations in Zn concentrations are in some cases not statistically significant. The possible increase in Zn concentration above the biochar+concrete material is likely caused by the high levels of Zn in the concrete slurry material (7 µg·L^{-1} released from control sample, Table 5). The uncapped columns and columns with biochar mixed into the sediment displays a significant decrease (about 57-60%) in Zn levels after 60 days. This is a general trend but is more visible for the columns with a more elevated initial level. The maximum allowed level of Zn in the assessment criteria is set to 1.1 µg·L^{-1}, which is exceeded in all columns except the biochar+bentonite clay columns.

4.4.3 Cadmium and lead

Figure 13 displays the average concentrations of Cd and Pb after 19, 33 and 60 days in the experimental columns. The black bars show the Cd levels and the green displays Pb levels.

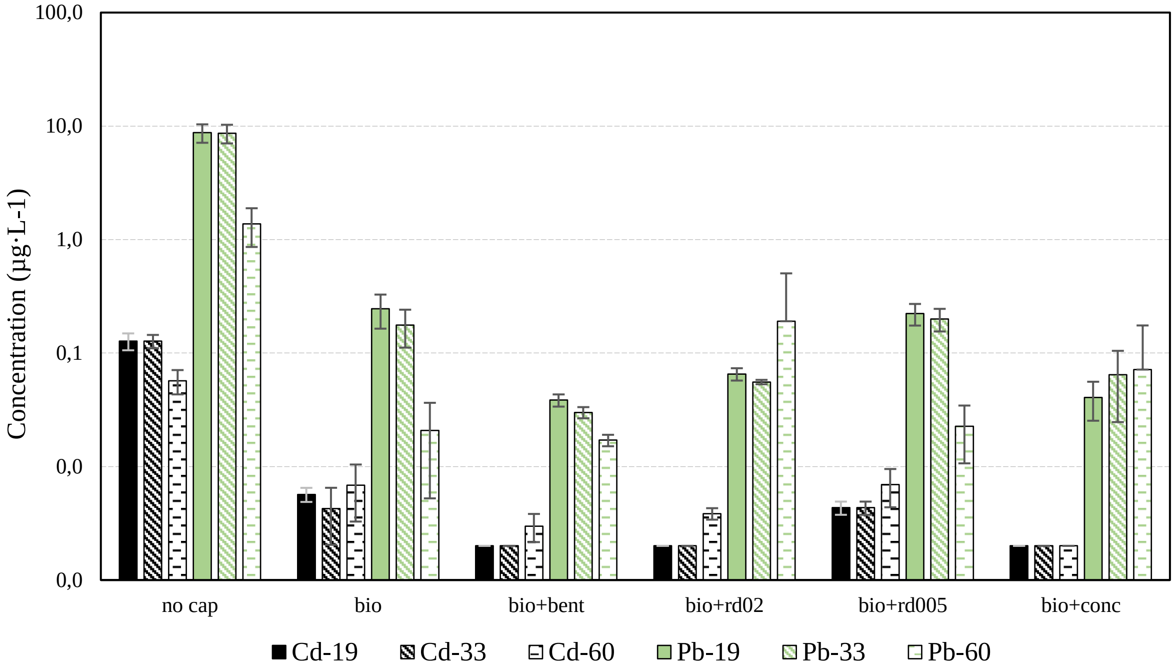

Fig 13. Average concentrations (µg·L^{-1}) for Cd and Pb over time in the water column above the uncapped and capped sediment in the column experiment. The samples were collected after 19, 33 and 60 days. Error bars show calculated SD.

Levels of Cd and Pb released into the water column are reduced for all capping materials. The most significant reduction of Cd is seen for the biochar+concrete layer which exhibits levels below the detection limit at all sampling occasions. Furthermore, it is evident that Pb levels are increasing with time in the rock dust of larger grain size. In Table 5, it can be observed that this material has slightly higher Pb levels initially. All capping materials, however, suggest efficient immobilization of Pb and Cd compared to levels in the uncapped columns. The low Cd levels may indicate either high TOC content and/or anoxic environment in the sediment as Cd generally is more mobile under oxidizing conditions at neutral pH.

4.4.4 Arsenic and phosphorus

Release of As from sediment to the water column is delayed when applying a capping layer on top of the sediment. However, As levels in uncapped columns (133 ± 30 µg·L^{-1}) and bentonite columns (41 ± 18 µg·L^{-1}) are considerably higher compared to the limit value of 1.1 µg·L^{-1} in coastal surface waters (HVFMS 2019:25). However, no estimated natural background levels have been found for levels of As in the Bothnian Bay, which should be accounted for when comparing to limit values. Average concentrations and calculated standard deviations (SD) for As and P (tot-P) levels over time are presented in Table 7 and Figure 14. The two elements are plotted together as they both are anions and were observed to follow the same trend for release through the capping materials. In Figure 15, the concentrations of As in the three biochar+bentonite clay columns over time are compared to the concentrations above the uncapped sediment and the alternative capping materials.

Table 7. Average concentrations (µg·L^{-1}) of As and P over time in the water column at 10 cm above the sediment and capping layers. Samples were collected after 19, 33 and 60 days. Standard deviations (µg·L^{-1}) were calculated for the triplicate columns at each sampling occasion.

	As-19	**As-33**	**As-60**	**SD-19**	**SD-33**	**SD-60**
no cap	181	190	133	67	66	30
bio	13	18	22	6	6	6
bio+bent	3	9	41	2	3	18
bio+rd02	30	38	48	6	6	3
Bio+rd005	15	19	36	5	8	6
bio+conc	0.2	0.3	1.4	0.1	0.1	0.4
	P-19	**P-33**	**P-60**	**SD-19**	**SD-33**	**SD-60**
no cap	62	48	29	16	9	18
bio	10	19	9	6	10	12
bio+bent	286	635	1052	77	75	260
bio+rd02	536	654	620	8	55	49
bio+rd005	238	556	385	99	392	95
bio+conc	1	1	1	0	0	0

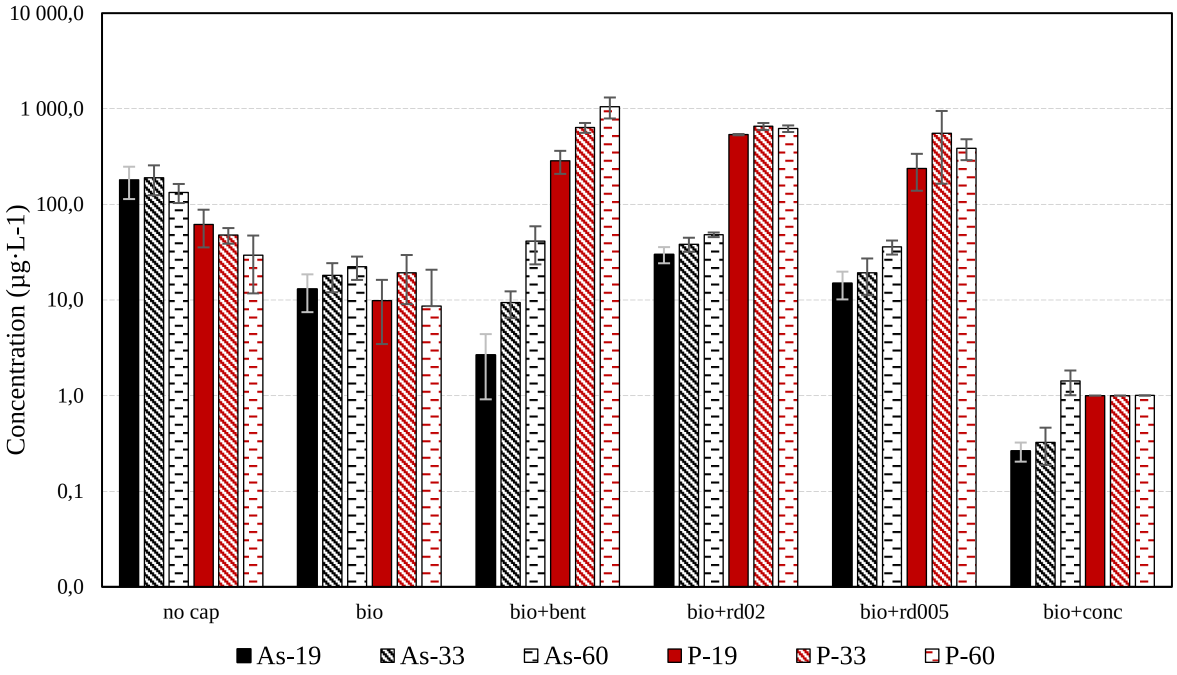

Fig 14. Average concentrations (µg·L^{-1}) for As and P over time in the water column above the uncapped and capped sediment in the experimental columns. The samples were collected after 19, 33 and 60 days. Error bars show calculated SD.

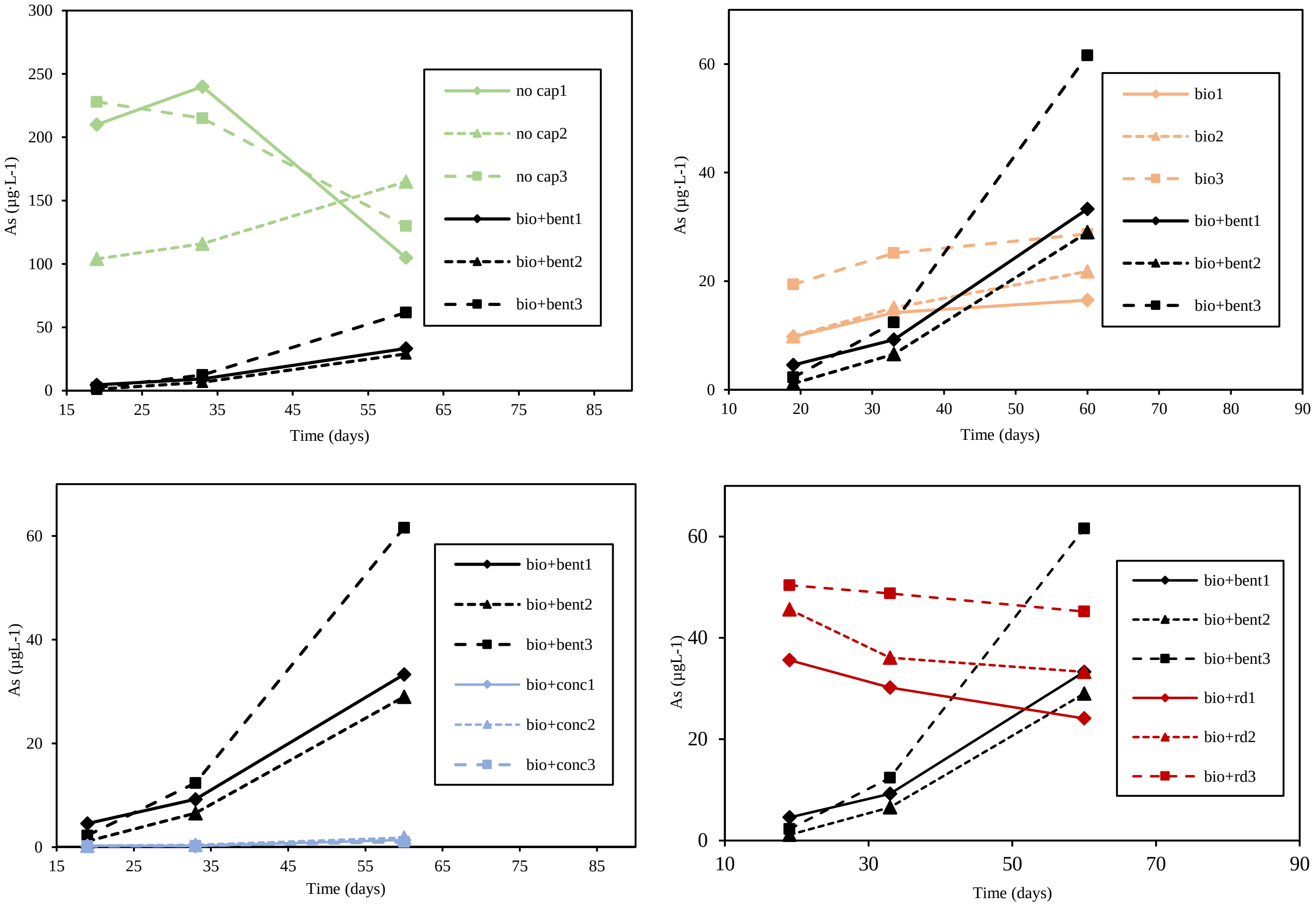

Fig 15. Concentration of As (µg·L^{-1}) in the water column above the biochar+bentonite clay compared to concentrations above uncapped sediment, biochar, biochar+concrete slurry and biochar+rockdust. The concentration in the triplicate columns for each material is presented and denoted 1, 2 and 3. Note that the rock dust presented is the coarse-grained (02) material as it displayed similar but slightly higher levels than the finer grained rock dust (005) for all measurements.

Figure 15 shows that the biochar+bentonite capping layer immobilized As at early stages of the experiment, followed by increased As concentration with time. The concentration of As increases approximately 2 times from 19 to 33 days, and continuously increases by about 300% from 33 to 60 days. The uncapped sediment, however, displays decreasing concentrations in two of the columns, and a clear trend cannot be distinguished. Furthermore, the lowest levels of As can be observed in the biochar+concrete layer columns (Figure 14). It is interesting to note that As levels are significantly lowered by the increasing pH (11.5) in the biochar+concrete columns. Generally, adsorption of anions decreases with increasing pH (Figure 15). The low levels above this capping layer could therefore suggest that As is adsorbed onto Fe-Mn oxides formed in the more oxidized surface layer. However, the overall increasing As and P levels with time (Figure 14) could suggest that the sediment and overlying water is getting more anoxic as oxygen gets depleted making As and P more mobile.

Levels of dissolved As and P show similar increases with time (Figure 14). Levels of dissolved P are observed to be high above the bentonite clay (1052 ± 260 $\mu g \cdot L^{-1}$) and rock dust materials (620 ± 49 $\mu g \cdot L^{-1}$ and 385 ± 95 $\mu g \cdot L^{-1}$) after 60 days (Table 7). However, as seen in Table 5 where the control samples are presented, these levels are most likely released from the added materials into the overlying water column. Nonetheless, dissolved As and P levels are increasing with time above all capping materials, but exhibits the lowest release for the biochar+concrete capping layer (Figure 14).

Diffusive fluxes of As were intended to be calculated in order to evaluate the diffusive release of As, but difficulties in pore water concentrations measurements made this calculation unreliable. Therefore, the diffusive behavior of As will only be assumed to delay the release of As for all capping materials.

4.5 Evaluation of the capping layers

To choose a suitable capping material for field application of a thin-layer cap, several factors need to be considered. Beyond the adsorption efficiency and isolation of contaminants, factors such as the price of the capping material, the ecological footprint and also the physicochemical aspects of the application should be considered. Additionally, the total cost of a material varies a lot depending on purchase price, cost of transport and management. Benefits with the alternative materials (concrete slurry and rock dust) are that they are residual products available in nearby areas resulting in reduced transport emissions and cost compared to the bentonite clay. However, the amount of bentonite clay needed in the laboratory experiment for a 2-4 cm thick layer (2 $kg \cdot m^{-2}$) was about 10 times less than the amount needed for the rock dust and concrete slurry (20 $kg \cdot m^{-2}$).

As discussed in the previous sections, all capping materials generally displays lower levels of As, Cd, Cu, Hg, Pb, Zn, Fe, Mn and SO_4 compared to the control columns with uncapped sediment. To gain a better understanding of which materials are most efficient at preventing release of a specific trace element, the maximum and minimum observed average levels in the columns after 19, 33 and 60 days for some of the elements are compiled in Table 8.

Table 8. Minimum and maximum average levels observed for selected trace elements in the columns after 19, 33 and 60 days. The maximum levels are marked with an H, and minimum levels with an L. *=below detection limit.

19 days	**As**	**P**	**Cd**	**Cu**	**Fe**	**Hg**	**Mn**	**Pb**	**Zn**	**SO_4**
Bio			H			*	H	H		
Bio+bent			*			*			L	H
Bio+rd02	H	H	*			*				
Bio+rd05			*	H	H	*				
Bio+conc	L	L	*	L	L	*	L*	L	L	L
33 days	**As**		**Cd**	**Cu**	**Fe**	**Hg**	**Mn**	**Pb**	**Zn**	**SO_4**
Bio			H			*	H		H	
Bio+bent			*			*		L	L	H
Bio+rd02	H	H	*			*				
Bio+rd05			*	H	H	*		H		
Bio+conc	L	L	*	L	L	*	L			L
60 days	**As**		**Cd**	**Cu**	**Fe**	**Hg**	**Mn**	**Pb**	**Zn**	**SO_4**
Bio			H			*	H			
Bio+bent		H	*		H	*			L	H
Bio+rd02	H		*			*		H		
Bio+rd05			*	H		H				
Bio+conc	L	L	*	L	L	*	L	L	H	L

The concrete slurry thin-layer cap has the highest efficiency for preventing release of trace elements from the sediment to the overlying water. However, it is important to note that the significant increase in pH in the overlying water body would not occur in field conditions, and that the retention of heavy metals would likely not be as efficient as in the laboratory set up. As the water in the columns was not replaced between the sampling occasions, all dissolved metals are remaining in the stagnant water, most likely resulting in an overestimation of dissolved levels which could contribute to a larger difference in levels between e.g., uncapped and capped sediment. Nonetheless, comparison between the capping layers can be considered as relatively reliable as they all have been exposed to the same experimental conditions and limitations.

The rock dust materials exhibit higher levels of released trace elements for As, Cu, Hg and Pb and can be considered less efficient than the bentonite clay or the concrete slurry. As mentioned previously, the rock dust of both grain sizes displayed difficulties of settling in the columns, which may be one contributor for the higher levels. Furthermore, the columns where biochar was mixed into the sediment shows higher levels of Cd and Mn compared to the other capping materials, indicating that the isolation factor provided by the 2-4 cm thick capping layers is beneficial for preventing release of trace elements from the sediment.

5 Conclusions

The experimental set up revealed that capping layers containing an active material mixed with a structural material effectively prevents release of trace elements trough the sediment to the overlying water (Figure 9 and 10). Evaluation of the different capping materials showed that the concrete slurry had the most suitable settling properties and negligible loss of biochar in the set-up of the columns. The biochar+concrete slurry thin-layer cap displayed the highest efficiency for preventing and/or delaying release of As, P, Cu, Fe, Mn and SO4 while higher levels ($7\ \mu g\cdot L^{-1}$) of Zn could be observed. Furthermore, Mercury and Cd displayed low levels in all the columns, most likely being bound to organic matter in the sediment.

An increase in pH and conductivity was observed in all columns (Figure 7). Biochar mixed in the sediment yielded a slight increase in pH (7.7) followed by the rock dust materials (8.1-8.2), bentonite clay layer (8.5) and the highest observed increase to a pH of 11.5 by the concrete slurry. However, it is important to note that, under field conditions, the overlying water in Burefjärden would not have this increase, but a slight increase in the sediment surface pH would most likely occur retaining metal cations.

Arsenic and P occurring as anionic species show similar trends of release through the different capping layers (Figure 14). Despite the observed increase in pH, the concrete slurry is most efficient at immobilizing As and P to levels of $1.4\ \mu g\cdot L^{-1}$ and $<1\ \mu g\cdot L^{-1}$, respectively. The most likely explanation would be that As and P are kept bound in sulfides (As) in the sediment and/or co-precipitated on Fe and Mn hydroxides (As and P) at the sediment-capping layer interface. Copper and Zn occurring as cations also display similar trends over time for all columns. The most noticeable difference is that Cu and Zn decreases with time while As and P increase with time in the columns.

The evaluation of the efficiency of these thin-layer capping materials was conducted in a laboratory set up without consideration of field conditions such as erosion, advective flows, seasonal changes and that the pH in the sea water is constant. Furthermore, levels of contaminants in sediment and their potential environmental risk are also affected by biota which can vary between different areas and change over time. Pilot-scale experiments and further research regarding field application of capping materials and effects on biota would therefore be essential.

6 References

Artioli, Y. (2008). *Encyclopedia of Ecology* (1 ed.). (B. Fath, & S. Jorgensen, Eds.) Elsevier Science. doi:https://doi.org/10.1016/B978-008045405-4.00252-4

Azcue, J., Zeman, A., & Förstner, U. (1998). International review of application of subaqueous capping techniques for remediation of contaminated sediments. *Environmental Geotechnics, 2*, 537-542.

Bourg, A., & Loch, J. (1995). Mobilization of Heavy Metals as Affected by pH and Redox Conditions. In Salomon, W. Salomons, & W. Stigliani, *Biogeodynamics of Pollutants in Soils and Sediments* (pp. 87-102). Springer, Berlin, Heidelberg. doi:https://doi.org/10.1007/978-3-642-79418-6_4

Cornelissen, G., Amstaetter, K., Hauge, A., Schaanning, M., Beylich, B., Gunnarsson, J., . . . Eek, E. (2012). Large-Scale Field Study on Thin-Layer Capping of Marine PCDD/F Contaminated Sediments in Grenlandfjords, Norway: Physicochemical Effects. *Environ. Sci. Technol., 46*, 12030-12037. doi:dx.doi.org/10.1021/es302431u

Cornelissen, G., Elmquist Kruså, M., Eek, E., Oen, A., Arp, H., Raymond, C., . . . Gunnarsson, J. (2011). Remediation of Contaminated Marine Sediment Using Thin-Layer Capping with Activated Carbon-A Field Experiment in Trondheim Harbor, Norway. *Environ. Sci. Technol., 45*, 6110-6116. doi:dx.doi.org/10.1021/es2011397

Dabrowski, A. (2001). Adsorption - from theory to practice. *Advances in Colloid and Interface Science, 93*(1-3), 135-224. doi:https://doi.org/10.1016/S0001-8686(00)00082-2

Gambrell, R., Wiesepape, J., & Patrick, W. (1991). The effects of pH, redox, and salinity on metal release from a contaminated sediment. *57*, 359-367. doi:https://doi.org/10.1007/BF00282899

Geo Innova. (2008). *Förnyad huvudstudie Scharings industriområde.* Skellefteå kommun. Retrieved from https://www.skelleftea.se/Kommunledningskontoret/Innehallssidor/Bifogat/Huvudrapport-reviderad-080529.pdf

Ghosh, U., Luthy, R., Cornelissen, G., Werner, D., & Menzie, C. (2011). In-situ Sorbent Amendments: A New Direction in Contaminated Sediment Management. *Environmental Science & Technology, 45*, 1163-1168. doi:dx.doi.org/10.1021/es102694h

HVFMS 2019:25. (2019). *Havs- och vattenmyndighetens föreskrifter om klassificering och miljökvalitetsnormer avseende ytvatten*. Retrieved from https://www.havochvatten.se/download/18.4705beb516f0bcf57ce1c145/1576576601249/HVMFS%202019-25-ev.pdf

Jersak, J., Göransson, G., Ohlsson, Y., Larsson, L., Flyhammar, P., & Lindh, P. (2016a). *In-situ capping of contaminated sediments - Sediment remediation technologies: A general overview.* Linköping: SGI. Retrieved from https://www.sgi.se/globalassets/publikationer/sgi-publikation/sgi-p30-7.pdf

Jersak, J., Göransson, G., Ohlsson, Y., Larsson, L., Flyhammar, P., & Lindh, P. (2016b). *In-situ capping of contaminated sediments. Remedial sediment capping projects, worldwide: A preliminary review.* Linköping: SGI. Retrieved from http://www.diva-portal.org/smash/get/diva2:1300112/FULLTEXT01.pdf

Joseph, S., Lehmann, J., & Earthscan from Routledge. (2015). *Biochar for Environmental Management: Science, Technology and Implementation* (2nd ed.). Routledge.

Kautsky, L., & Kautsky, N. (2000). The Baltic Sea, including Bothnian Sea and Bothnian Bay. In C. Sheppard, *Seas at the millennium: an environmental evaluation: 1. Regional chapters: Europe, The Americas and West Africa* (pp. 121-133).

Knox, A., Paller, M., & Dixon, K. (2014). Evaluation of Active Cap Materials for Metal Retention in Sediments. *Remediation Journal, 24*(3), 49-69. doi:https://doi.org/10.1002/rem.21394

Länsstyrelsen. (n.d.). *Förorenade områden i Västerbotten.* Retrieved from https://www.lansstyrelsen.se/vasterbotten/miljo-och-vatten/fororenade-omraden/fororenade-omraden-i-lanet.html#0

Lehoux, A., Petersen, K., Leppänen, M., Snowball, I., & Olsen, M. (2020). Status of contaminated marine sediments in four Nordic countries: assessments, regulations, and remediation approaches. *Journal of Soils and Sediments, 20*, 2619-2629. doi:https://doi.org/10.1007/s11368-020-02594-3

MRCCC. (n.d.). *Water quality standards*. Retrieved from https://mrccc.org.au/wp-content/uploads/2013/10/Water-Quality-Salinity-Standards.pdf

Naturvårdsverket. (1999). *Bedömningsgrunder för miljökvalitet, Kust och hav. Rapport nr 4914.*

Naturvårdsverket. (2003). *Efterbehandling av förorenade sediment - en vägledning.* Retrieved from https://www.naturvardsverket.se/Documents/publikationer/620-5254-3.pdf

Naturvårdsverket. (2020a). *Förorenade sediment.* Retrieved from https://www.naturvardsverket.se/Miljoarbete-i-samhallet/Miljoarbete-i-Sverige/Uppdelat-efter-omrade/Fororenade-omraden/Fororenade-sediment/

Naturvårdsverket. (2020b). *Rönnskärsverken - följ ärendet.* Retrieved from https://www.naturvardsverket.se/Stod-i-miljoarbetet/Rattsinformation/Rattsfall/Metallindustri/Ronnskarsverken/

O'day, P. (2006). Chemistry and Mineralogy of Arsenic. *Elements, 2*(2), pp. 77-83.

Olsen, M., Petersen, K., Lehoux, A., Leppänen, M., Schaanning, M., Snowball, I., . . . Lund, E. (2019). *Contaminated Sediments: Review of solutions for protecting aquatic environments.* Nordic Council of Ministers. Retrieved from http://www.diva-portal.org/smash/get/diva2:1336098/FULLTEXT01.pdf

Peng, J.-F., Song, Y.-H., Yuan, P., Cui, X.-Y., & Qui, G.-L. (2009). The remediation of heavy metals contaminated sediments. *Journal of Hazardous Materials, 161*(2-3), 633-640. doi:https://doi.org/10.1016/j.jhazmat.2008.04.061

Ramboll. (2019a). *Miljöteknisk sedimentundersökning, Bureå träsliperi.*

Ramboll. (2019b). *Huvudstudie Bureå Träsliperi: åtgärdsmetoder för sediment och fiberbankar.*

Regeringen. (2019). Uppdrag om förbättrad kunskap för hantering av förorenade sediment. Retrieved from https://www.naturvardsverket.se/upload/miljoarbete-i-samhallet/miljoarbete-i-sverige/regeringsuppdrag/2019/fororenade-sediment-regeringsuppdrag.pdf

Søndergaard, M. (2009). Redox potential. In G. Likens (Ed.), *Encyclopedia of Inland Waters* (pp. 852-859). Academic Press. doi:https://doi.org/10.1016/B978-012370626-3.00115-0

Severin, M., Josefsson, S., Nilsson, P., Ohlsson, Y., Stjärne, A., & Wernersson, A.-S. (2018). *Förorenade sediment - behov och färdplan för en renare vattenmiljö.* SGU Rapport 2018:21. Retrieved from http://resource.sgu.se/produkter/sgurapp/s1821-rapport.pdf

SGF (Svenska Geotekniska Föreningen). (2018). *Åtgärdsportalen*. Retrieved from Klassisk in situ-behandling - Fördjupning: https://atgardsportalen.se/metoder/sediment/insitu-sediment/klassisk-in-situ-behandling/klassisk-insitu-fordjupn

SGF (Svenska Geotekniska Föreningen). (2019). *Muddringsmetoder - Översikt*. Retrieved from Åtgärdsportalen: https://atgardsportalen.se/metoder/sediment/ex-situ-muddring/muddringsmetoder

SGF (Svenska Geotekniska Föreningen). (2020). *Efterbehandling av sediment*. Retrieved from Åtgärdsportalen: https://atgardsportalen.se/metoder/sediment

SGU. (2016). *Kartläggning och riskklassning av fiberbankar i Norrland.* SGU. Retrieved from https://resource.sgu.se/produkter/sgurapp/s1621-rapport.pdf

Skellefteå kommun. (2020). *Fd Bureå AB.* Retrieved from https://www.skelleftea.se/fd-burea-ab

Thomas, E., Borchard, N., Sarmiento, C., Atkinson, R., & Labb, B. (2020). Key factors determining biochar sorption capacity for metal contaminants: a literature synthesis. *Biochar, 2*, 151-163. doi:https://doi.org/10.1007/s42773-020-00053-3

Wang, J., & Wang, S. (2019). Preparation, modification and environmental application of biochar: A review. *Journal of Cleaner Production, 227*, 1002-1022. doi:https://doi.org/10.1016/j.jclepro.2019.04.282

Wang, M., Zhu, Y., Cheng, L., Anderson, B., Zhao, X., Wang, D., & Ding, A. (2018). Review on utilization of biochar for metal-contaminated soil and sediment remediation. *Journal of Environmental Sciences, 63*, 156-173. doi:http://dx.doi.org/10.1016/j.jes.2017.08.004

Wang, S., & Peng, Y. (2010). Natural zeolites as effective adsorbents in water and wastewater treatment. *Chemical Engineering Journal, 156*, 11-24. doi:https://doi.org/10.1016/j.cej.2009.10.029

VISS. (2020). Retrieved from VER, fria vattenmassan kust, Västerbottens län: https://viss.lansstyrelsen.se/MonitoringPrograms.aspx?monitoringProgramID=492&tab=Surveys&managementCycleName=Cykel_2#tabSurveys

VISS. (n.d.). *Burefjärden: Förvaltningscykel 3.* Retrieved from https://viss.lansstyrelsen.se/Waters.aspx?waterMSCD=WA77389916&managementCycleName=Senaste_bedoemning

Yang, Y., Ye, S., Zhang, C., Zeng, G., Tan, X., Song, B., . . . Chen, Q. (2020). Application of biochar for the remediation of polluted sediments. *Journal of Hazardous Materials, 404*(Part A). doi:https://doi.org/10.1016/j.jhazmat.2020.124052.

Zhang, C., Yu, Z.-G., Zeng, G.-M., Jiang, M., Yang, Z.-Z., Cui, F., . . . Hu, L. (2014). Effects of sediment geochemical properties on heavy metal bioavailability. *Environment International, 73*, 270-281. doi:https://doi.org/10.1016/j.envint.2014.08.010.

Zhang, C., Zhu, M.-Y., Zeng, G.-M., Yu, Z.-G., Cui, F., Yang, Z.-Z., & Shen, L.-Q. (2016). Active capping technology: a new environmental remediation of contaminated sediment. *Environmental Science and Pollution Research, 23*, 4370-4386. doi:https://doi.org/10.1007/s11356-016-6076-8

Appendix A: Photos of sediment and materials

Sediment collected from the Bureå sea area

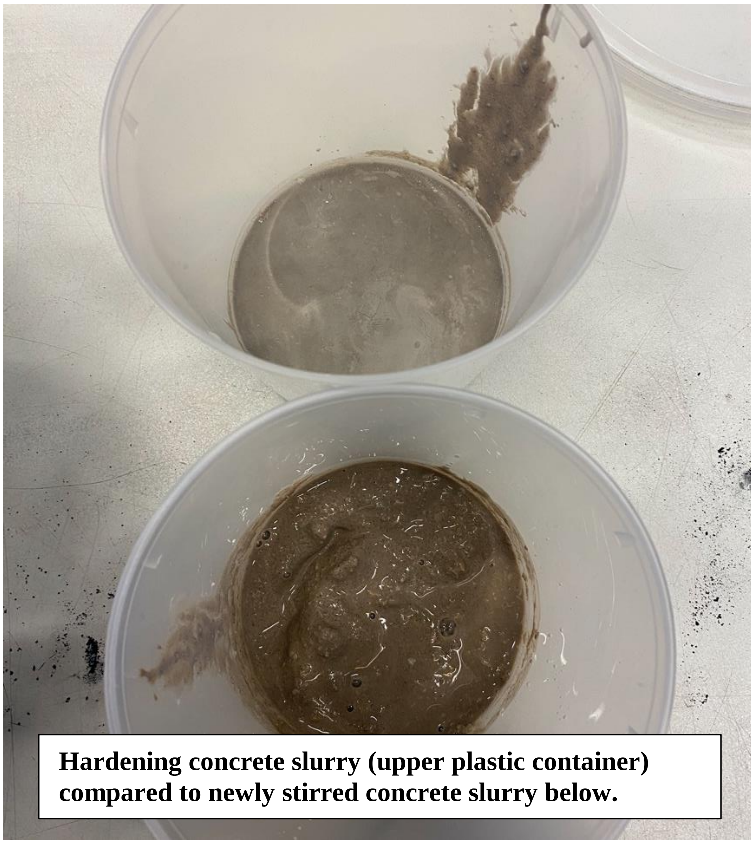

Hardening concrete slurry (upper plastic container) compared to newly stirred concrete slurry below.

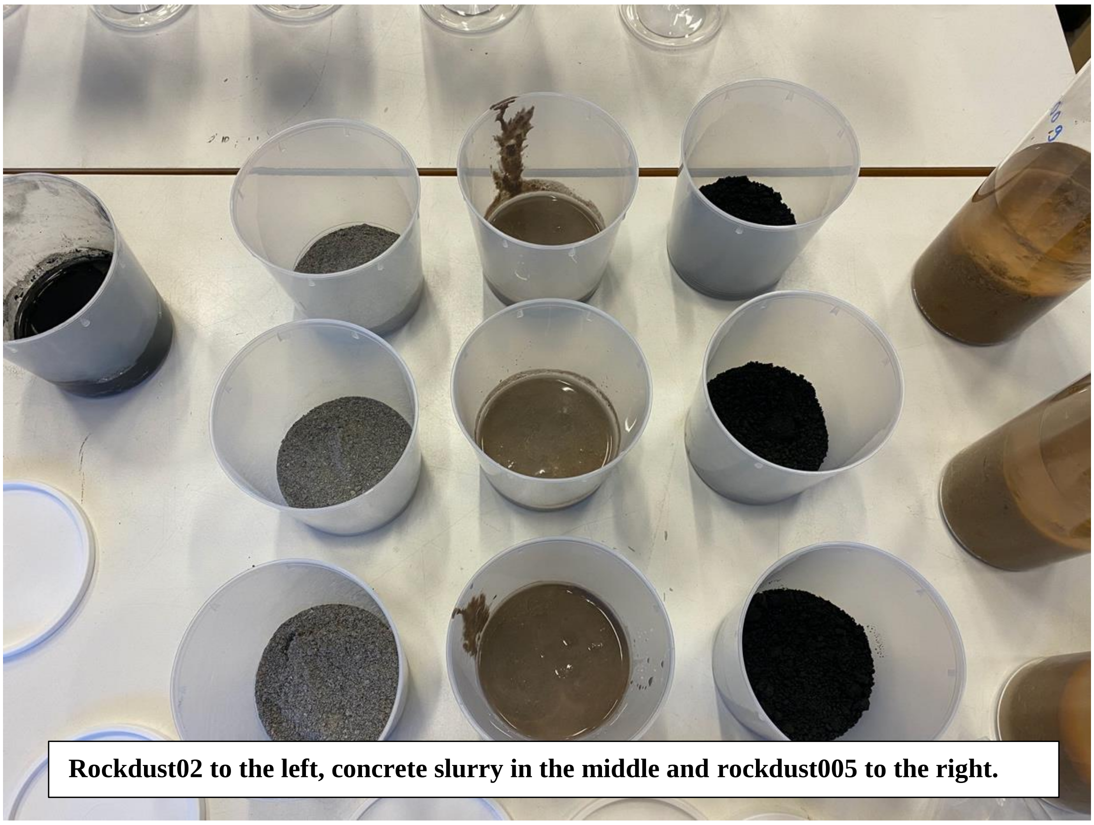

Rockdust02 to the left, concrete slurry in the middle and rockdust005 to the right.

Appendix B: Complete analysis protocols

Analysis Date:	**2021-03-12**			
ELEMENT	SAMPLE	Stenmjöl 0-2	Stenmjöl 0-005	Betongslam
Sampling Date		2021-02-17	2021-02-17	2021-02-17
Siktning/mortling		Ja	Ja	Ja
Torkning		Ja	Ja	Ja
Uppslutning		Ja	Ja	Ja
As, arsenik	mg/kg TS	5,88	0,646	4,18
Ba, barium	mg/kg TS	126	266	122
Cd, kadmium	mg/kg TS	<0.1	<0.1	0,317
Co, kobolt	mg/kg TS	18,6	9,96	5,46
Cr, krom	mg/kg TS	57,2	32,5	26,3
Cu, koppar	mg/kg TS	66	13,3	36
Hg, kvicksilver	mg/kg TS	<0.2	<0.2	<0.2
Ni, nickel	mg/kg TS	33	7,89	13,5
Pb, bly	mg/kg TS	12,2	2,95	12,1
V, vanadin	mg/kg TS	95,1	62,4	44,3
Zn, zink	mg/kg TS	89,8	89,3	468
Torrsubstans vid 105°C	%	85,1	99,8	37,2

Analysis Date:	**2021-03-16**																			
ELEMENT	SAMPLE	Lövskär	S1	S2	S3	SB1	SB2	SB3	SBBE1	SBBE2	SBBE3	SBST1	SBST2	SBST3	SBC1	SBC2	SBC3	SBF1	SBF2	SBF3
Sampling Date		2021-03-08	2021-03-08	2021-03-08	2021-03-08	2021-03-08	2021-03-08	2021-03-08	2021-03-08	2021-03-08	2021-03-08	2021-03-08	2021-03-08	2021-03-08	2021-03-08	2021-03-08	2021-03-08	2021-03-08	2021-03-08	2021-03-08
Al, aluminium	µg/L	31	28,7	29,8	33,2	9,52	9,71	11,1	26,3	38,1	34,8	20	17,6	17,8	5,25	2,06	7,81	41,5	55,4	76,2
As, arsenik	µg/L	0,193	210	104	228	9,76	9,85	19,4	4,56	1,14	2,27	35,6	30,2	24,1	0,292	0,303	0,195	10,9	20,3	13,7
Ba, barium	µg/L	10,1	10,3	9,22	11,3	14,6	14,4	13,2	7,32	7,99	7,74	10,5	10,1	10,1	270	241	109	11,3	8	8,84
Ca, kalcium	mg/L	5,3	15,7	13,6	16,4	14,2	13,8	12,6	5,86	6,18	5,87	7,62	7,53	7,23	87	112	31,4	10,4	10,5	11,6
Cd, kadmium	µg/L	0,0123	0,125	0,107	0,15	0,0056	0,0065	0,0049	<0.002	<0.002	<0.002	<0.002	<0.002	<0.002	<0.002	<0.002	<0.002	<0.004	<0.004	<0.005
Co, kobolt	µg/L	0,0875	0,0895	0,0379	0,216	0,0392	0,0239	0,0291	0,0127	0,0176	0,0198	0,0169	0,0104	0,0121	0,0109	0,0059	0,0057	0,0306	0,0504	0,061
Cr, krom	µg/L	0,148	0,179	0,156	0,212	0,0547	0,134	0,0975	0,153	0,134	0,137	0,128	0,117	0,113	0,469	0,287	0,215	0,177	0,162	0,186
Cu, koppar	µg/L	0,77	2,35	2,29	2,79	0,664	0,625	0,684	0,348	0,297	0,308	0,25	0,311	0,328	0,314	0,28	0,253	1,2	0,721	1,1
Fe, järn	mg/L	0,222	0,38	0,63	0,338	0,0674	0,0669	0,0704	0,061	0,0638	0,0725	0,0689	0,0586	0,066	0,0012	<0.0004	<0.0004	0,088	0,0746	0,0915
Hg, kvicksilver	µg/L	<0.002	0,0073	0,0064	0,0107	<0.002	<0.002	<0.002	<0.002	<0.002	<0.002	<0.002	<0.002	<0.002	<0.002	<0.002	<0.002	<0.002	<0.002	<0.002
K, kalium	mg/L	1,77	7,44	6,62	7,83	17,3	17,6	20,3	12,3	10	8,87	39,2	38,1	37,6	58,8	41,2	53,8	36,7	40,2	38,8
Mg, magnesium	mg/L	3,67	10,5	8,95	11	10,5	10,3	9,65	5,19	5,36	5,06	6,06	6,58	6,4	1,03	0,807	2,06	6,35	6,98	6,92
Mn, mangan	µg/L	17,4	287	200	336	151	168	128	1,47	1,8	1,51	1,01	0,69	2,06	<0.03	<0.03	<0.03	5,47	10,5	10,3
Mo, molybden	µg/L	0,686	4,34	2,9	4,66	2,09	2,13	2,5	2,03	1,64	1,57	1,99	1,72	1,69	1,14	1,23	0,912	10,3	8,87	9,69
Na, natrium	mg/L	30,9	125	107	131	117	114	110	562	429	361	93,4	94	95	86,6	91,4	82,3	84,1	88,2	94
Ni, nickel	µg/L	0,462	0,639	0,519	0,724	0,389	0,335	0,33	0,226	0,269	0,251	0,377	0,25	0,266	0,0693	0,0556	0,0536	0,349	0,27	0,277
P, fosfor	µg/L	3,05	67,8	33	84,4	5,05	7,4	17,1	373	226	258	527	538	543	<1	<1	<1	126	315	274
Pb, bly	µg/L	0,143	7,76	10,6	7,85	0,336	0,224	0,177	0,0341	0,0378	0,0435	0,0747	0,0612	0,0601	0,0582	0,0328	0,0308	0,171	0,231	0,266
Si, kisel	mg/L	1,62	3,87	3,12	3,99	2,85	2,83	2,74	1,84	1,79	1,79	2,17	2,09	2,01	1,84	1,71	1,7	1,95	2,18	2,2
Sr, strontium	µg/L	38,8	203	168	213	171	164	148	67,2	67,2	63	72,8	73,6	70,3	758	575	341	72	80,4	79
V, vanadin	µg/L	1,83	1,8	1,65	1,88	0,8	0,88	0,864	8,5	5,18	5,9	1,59	1,25	1,28	1,05	1,02	0,823	2,14	1,53	1,69
Zn, zink	µg/L	2,3	3,76	3,76	3,74	1,69	2,4	2,66	0,508	1,22	0,733	1,27	1,4	1,41	0,765	0,867	0,806	1,47	0,713	1,14
klorid	mg/L	49,2	203	178	188	195	189	183	752	574	479	147	148	148	92,2	127	76	131	136	147
SO4, sulfat	mg/L	11,2	23,9	20	24,1	30,5	26,6	25,9	55,9	45,6	45,1	19,7	20,3	19,7	8,1	8,34	7,32	25,4	25,2	25,4

Analysis Date	**2021-04-12**																		
ELEMENT	SAMPLE	S1	S2	S3	SB1	SB2	SB3	SBBE1	SBBE2	SBBE3	SBST1	SBST2	SBST3	SBC1	SBC2	SBC3	SBF1	SBF2	SBF3
Sampling Date		2021-03-22	2021-03-22	2021-03-22	2021-03-22	2021-03-22	2021-03-22	2021-03-22	2021-03-22	2021-03-22	2021-03-22	2021-03-22	2021-03-22	2021-03-22	2021-03-22	2021-03-22	2021-03-22	2021-03-22	2021-03-22
Al, aluminium	µg/L	29,1	27	32,7	8,39	8,14	9,04	6,34	6,31	6,32	17,6	17,9	19,8	34,3	19,2	21,4	32,9	33,4	42
As, arsenik	µg/L	240	116	215	14,2	15,1	25,2	9,21	6,56	12,4	45,6	36,1	33,3	0,225	0,481	0,269	16,4	28,2	13
Ba, barium	µg/L	10,8	8,75	10,9	14,9	14,3	12,9	7,41	7,23	7,07	10,4	10,1	10,2	302	304	268	11,6	8,2	8,03
Ca, kalcium	mg/L	17,5	14,5	17,6	15,9	16,2	15,3	5,82	5,76	4,94	8,87	8,33	8,62	88,1	192	94,6	12,6	13,4	12,1
Cd, kadmium	µg/L	0,119	0,116	0,147	0,0065	0,0044	<0.002	<0.002	<0.002	<0.002	<0.002	<0.002	<0.002	<0.002	<0.002	<0.002	<0.004	<0.005	<0.004
Co, kobolt	µg/L	0,0797	0,0272	0,144	0,0236	0,0138	0,0175	0,0107	0,0098	0,0101	0,0145	0,0445	0,0177	0,0078	0,0122	0,0112	0,0281	0,031	0,0476
Cr, krom	µg/L	0,232	0,19	0,203	0,104	0,0893	0,105	0,13	0,11	0,119	0,129	0,109	0,117	0,488	0,319	0,245	0,141	0,122	0,133
Cu, koppar	µg/L	2,67	2,67	3,38	0,702	0,612	0,681	0,408	0,311	0,377	0,339	0,367	0,35	0,206	0,249	0,243	1,4	0,862	1,1
Fe, järn	mg/L	0,446	0,673	0,322	0,0592	0,0513	0,0594	0,0449	0,04	0,0479	0,0606	0,0518	0,0602	0,0006	0,0011	0,0014	0,0774	0,0439	0,0599
Hg, kvicksilver	µg/L	0,0076	0,0047	0,0105	<0.002	<0.002	<0.002	<0.002	<0.002	<0.002	<0.002	<0.002	<0.002	<0.002	0,0029	<0.002	<0.002	<0.002	<0.004
K, kalium	mg/L	8,64	7,65	8,79	23,3	26	28,8	14,6	14,6	11,8	42,5	42,5	42,4	68,9	41,7	59,7	42,6	46,8	40,9
Mg, magnesium	mg/L	11,8	9,66	11,8	11,6	12	11,4	5,31	5,29	4,39	7,06	7,18	7,41	0,141	0,163	0,568	7,52	8,54	7,23
Mn, mangan	µg/L	354	222	363	183	215	161	1,32	1,17	0,519	0,964	0,546	1,43	<0.03	0,0368	<0.03	10	17,5	10,4
Mo, molybden	µg/L	4,19	2,78	4,41	2,19	2,19	2,64	2,56	2,71	2,64	2,16	1,8	1,92	0,935	1,64	0,994	11,3	9,88	9,33
Na, natrium	mg/L	138	118	145	138	141	140	640	637	490	111	112	116	103	104	96,4	105	115	101
Ni, nickel	µg/L	0,677	0,6	0,818	0,409	0,393	0,336	0,193	0,239	0,254	0,262	0,206	0,346	<0.05	<0.05	0,0782	0,414	0,173	0,341
P, fosfor	µg/L	55,6	38,1	49,3	9,2	19	29,7	637	559	709	679	591	693	<1	<1	<1	<1000	412	257
Pb, bly	µg/L	8,32	10,4	7,22	0,251	0,141	0,137	0,0281	0,028	0,0339	0,0582	0,0552	0,0533	0,0637	0,105	0,0251	0,173	0,175	0,252
Si, kisel	mg/L	4,51	3,38	4,2	3,36	3,66	3,54	2	1,95	1,8	2,51	2,33	2,37	3,4	2,81	2,61	2,26	2,59	2,24
Sr, strontium	µg/L	230	184	232	196	203	186	71	70,4	59,9	92,6	86,3	89,1	808	638	811	90,1	105	83,6
V, vanadin	µg/L	1,88	1,72	1,88	0,765	0,73	0,755	11,6	11,4	11,4	1,53	1,33	1,36	0,555	0,796	0,564	2,64	1,67	1,72
Zn, zink	µg/L	3,61	3,29	3,65	2,28	2,72	2,54	0,808	0,87	0,652	1,45	1,38	1,61	1,14	1,07	1,34	1,39	0,751	0,998
klorid	mg/L	233	201	230	230	235	218	936	923	773	183	173	186	101	179	105	170	180	162
SO4, sulfat	mg/L	24,4	19,9	24,3	33,3	30,9	30,2	72,4	70,7	69,7	23,2	23	19,3	6,18	7,64	7,17	26,7	30,1	24,9

Analysis Date	**2021-05-12**																		
ELEMENT	SAMPLE	S1	S2	S3	SB1	SB2	SB3	SBBE1	SBBE2	SBBE3	SBST1	SBST2	SBST3	SBC1	SBC2	SBC3	SBF1	SBF2	SBF3
Sampling Date		2021-04-28	2021-04-28	2021-04-28	2021-04-28	2021-04-28	2021-04-28	2021-04-28	2021-04-28	2021-04-28	2021-04-28	2021-04-28	2021-04-28	2021-04-28	2021-04-28	2021-04-28	2021-04-28	2021-04-28	2021-04-28
Al, aluminium	µg/L	18,9	6,03	6,38	3,77	3,06	2,93	5,71	5,25	5,08	14,2	12,9	13,2	214	149	148	23,5	25,1	26,5
As, arsenik	µg/L	105	165	130	16,5	21,8	28,7	33,3	29	61,6	50,4	48,8	45,2	1,4	1,84	1,02	32,5	42,8	32,3
Ba, barium	µg/L	6,38	1,88	5,59	10,8	10,5	8,99	8,82	9,4	9,52	13,7	14	15,6	475	266	269	15	9,23	11,6
Ca, kalcium	mg/L	22,3	19,6	22,6	20,8	21,2	19,1	6,39	6,34	6,01	14,9	14,7	17,8	174	192	50,1	20,1	18,4	20,8
Cd, kadmium	µg/L	0,0644	0,0411	0,0655	0,0103	0,0071	0,0032	0,0025	0,0025	0,004	0,0034	0,0043	0,0039	<0.002	<0.002	<0.002	0,0087	<0.004	0,0081
Co, kobolt	µg/L	0,0932	0,0244	0,103	0,0135	0,0141	0,0104	0,006	0,0099	0,0061	0,0094	0,0117	0,0154	0,0097	0,0062	0,0069	0,0229	0,012	0,0136
Cr, krom	µg/L	0,143	0,0417	0,101	0,0694	0,0543	0,0551	0,0991	0,0948	0,0836	0,0449	0,0525	0,0272	0,551	0,327	0,256	0,0752	0,0598	0,0693
Cu, koppar	µg/L	2,86	1,63	2,59	0,55	0,408	0,569	0,222	0,26	0,302	0,233	0,235	0,445	0,2	0,136	0,105	0,917	0,442	0,53
Fe, järn	mg/L	0,124	0,0967	0,0517	0,0089	0,0063	0,0037	0,0161	0,0207	0,015	0,0048	0,0036	0,0011	<0.0004	0,0011	<0.0004	0,0134	0,0036	0,0031
Hg, kvicksilver	µg/L	0,0024	<0.002	<0.002	<0.002	<0.002	<0.002	<0.002	<0.002	<0.002	<0.002	<0.002	<0.002	<0.002	<0.02	<0.002	<0.002	<0.002	<0.002
K, kalium	mg/L	9,92	10	10	32,9	36,4	37,2	19,3	19,3	18,6	48,5	47,3	48,2	72,6	49,2	68,8	47,6	53,6	47,9
Mg, magnesium	mg/L	14,4	12,6	14,4	13,8	14,3	12,9	5,52	5,52	5,08	10,2	10,5	12,6	<0.09	<0.09	<0.09	10,7	10,5	11
Mn, mangan	µg/L	88,1	196	220	71,5	161	1,54	0,296	0,298	0,116	0,846	1,13	3,11	0,0406	0,1	0,0392	2,03	0,317	4,64
Mo, molybden	µg/L	2,89	2,1	3,21	1,95	1,7	2,3	2,55	2,67	3,05	2,03	1,84	1,92	1,42	2,81	1,2	12,5	10,9	11
Na, natrium	mg/L	176	166	179	179	188	173	812	787	746	166	163	179	133	143	132	154	153	157
Ni, nickel	µg/L	0,856	0,451	0,672	0,333	0,287	0,209	0,16	0,191	0,192	0,173	0,207	0,234	0,0602	<0.05	0,0564	0,387	0,21	0,244
P, fosfor	µg/L	38,8	40,6	9,01	1,43	22,6	1,85	933	872	1350	590	594	677	<1	1,01	<1	290	480	385
Pb, bly	µg/L	1,85	1,44	0,83	0,0387	0,0138	<0.01	0,018	0,0184	0,0148	<0.01	0,552	<0.01	0,191	<0.01	0,0136	0,0363	0,0154	0,016
Si, kisel	mg/L	4,64	1,72	2,27	3,27	4,06	3,06	2,58	2,45	2,84	3,24	2,81	3,28	4,53	3,8	3,99	2,3	2,08	2,74
Sr, strontium	µg/L	289	248	291	251	265	231	81,7	78,9	79,1	160	159	194	640	384	335	140	138	146
V, vanadin	µg/L	1,23	0,773	0,679	0,559	0,474	0,59	15,5	14,4	19,3	1,63	1,42	1,55	0,132	0,134	0,072	3,41	1,99	2,74
Zn, zink	µg/L	2,12	0,628	1,71	0,726	0,907	0,828	0,564	0,396	0,844	0,685	0,752	0,769	1,9	0,862	0,831	0,927	0,507	0,508
klorid	mg/L	262	255	274	280	285	263	1130	1080	998	244	249	267	152	224	129	238	227	241
SO4, sulfat	mg/L	42,7	21,1	42,6	46,1	44,5	46,6	76,4	74,9	84,8	22,3	23,4	22	<5.00	<5.00	<5.00	29,3	28,8	27,6

Analysis Date	**2021-05-12**								
ELEMENT	SAMPLE	BE-contr1	BE-contr2	ST-contr1	ST-contr2	F-contr1	F-contr2	C-contr1	C-contr2
Sampling Date		2021-04-28	2021-04-28	2021-04-28	2021-04-28	2021-04-28	2021-04-28	2021-04-28	2021-04-28
Al, aluminium	µg/L	1,14	3,96	160	146	42,6	43,1	144	125
As, arsenik	µg/L	407	464	2,23	1,74	12,6	12,3	0,367	0,33
Ba, barium	µg/L	15,8	19	7,06	9,92	25,4	9,44	3190	2930
Ca, kalcium	mg/L	15,2	19,1	14,2	16,2	32,6	32,5	702	683
Cd, kadmium	µg/L	0,0074	<0.004	0,0044	0,0082	<0.03	<0.03	0,0032	0,0037
Co, kobolt	µg/L	0,268	0,179	0,0835	0,15	0,142	0,115	0,166	0,151
Cr, krom	µg/L	0,0823	0,151	0,0707	0,0164	0,168	0,156	4,04	3,65
Cu, koppar	µg/L	3,67	5,11	0,522	0,639	5,17	4,62	3,02	2,25
Fe, järn	mg/L	0,0013	0,006	0,0056	0,0033	0,0013	0,0023	0,0008	<0.0004
Hg, kvicksilver	µg/L	<0.002	<0.002	<0.002	<0.002	<0.002	<0.002	<0.002	<0.002
K, kalium	mg/L	9,48	10,2	16,7	18	18,2	18,4	165	164
Mg, magnesium	mg/L	9,39	11,2	1,65	1,98	7,26	7,34	<0.09	<0.09
Mn, mangan	µg/L	0,83	0,313	13,5	23,5	56,4	40,8	0,278	0,2
Mo, molybden	µg/L	5,82	5,95	5,48	5,62	69,3	67,7	4,29	3,9
Na, natrium	mg/L	1210	1280	12,2	12,8	12,1	12,8	78,3	77,1
Ni, nickel	µg/L	0,357	0,53	0,067	0,123	0,364	0,284	0,228	0,264
P, fosfor	µg/L	1320	1570	6,61	3,16	171	169	4,37	2,31
Pb, bly	µg/L	<0.01	0,27	0,093	0,117	0,0305	0,0147	3,1	2,93
Si, kisel	mg/L	6,88	7,43	2,74	2,88	5,79	5,85	0,166	0,148
Sr, strontium	µg/L	257	310	85,8	98,8	124	125	7800	7490
V, vanadin	µg/L	19,2	20	5,47	5,34	6,32	6,14	0,154	0,113
Zn, zink	µg/L	0,41	16,6	1,17	2,06	0,673	0,761	7,17	6,77
klorid	mg/L	1440	1520	3,72	3,86	7,62	7,64	4,33	4,33
SO4, sulfat	mg/L	225	226	25,5	25,3	67,6	67,9	<5.00	<5.00

Appendix C: pH and conductivity measurements

pH measurements in columns						
Date	2021-03-03	2021-03-10	2021-03-22	2021-04-01	2021-04-12	2021-04-23
Time (days)	4	10	22	32	43	55
Temp °C	17,3	17,8	18,1	18,2	18,2	18,1
S1	7,36	7,45	7,54	7,5	7,76	7,87
S2	7,34	7,4	7,48	7,43	7,8	7,97
S3	7,32	7,48	7,54	7,46	7,72	7,66
SB1	7,66	7,55	7,58	7,63	7,86	7,94
SB2	7,65	7,54	7,57	7,61	7,65	7,46
SB3	7,66	7,58	7,6	7,72	7,84	8,08
SBBE1	7,94	8,29	8,38	9,13	8,32	8,18
SBBE2	7,89	8,25	8,34	9	8,64	8,3
SBBE3	7,94	8,53	8,55	8,98	8,88	8,56
SBST1	8,08	8,01	8,06	7,85	7,98	8,19
SBST2	8,05	8,05	8,08	7,83	8,05	8,18
SBST3	8,05	8,08	8,1	7,92	8,1	8,15
SBC1	11,32	11,2	11,25	11,98	11,85	11,5
SBC2	11,58	11,15	11,43	11,94	11,76	11,49
SBC3	11,26	11,06	11,44	11,84	11,8	11,29
SBF1	8,15	8,18	8,11	7,83	8,1	8,27
SBF2	8,14	8,2	8,02	7,91	8,18	8,34
SBF3	8,1	8,15	8,08	7,86	8,28	8,2

pH measurements in columns						
Date	2021-03-03	2021-03-10	2021-03-22	2021-04-01	2021-04-12	2021-04-23
Time (days)	4	10	22	32	43	55
Temp °C	17,3	17,8	18,1	18,2	18,2	18,1
S1	849	828	834	977	1003	1102
S2	673	670	743	819	964	998
S3	863	855	898	978	1034	1367
SB1	845	834	925	1012	1098	1151
SB2	823	806	878	1015	1230	1253
SB3	786	786	824	948	1104	1340
SBBE1	1628	1993	1842	3390	3870	4100
SBBE2	1628	1993	1842	3390	3870	4100
SBBE3	1482	1823	1835	3340	3900	4120
SBST1	688	700	686	865	910	1051
SBST2	700	694	674	836	1011	997
SBST3	684	703	686	885	934	1113
SBC1	734	779	984	1387	1472	1475
SBC2	659	1112	1334	1629	1624	1586
SBC3	666	797	1012	1305	1403	1386
SBF1	647	646	786	867	953	1154
SBF2	666	662	814	879	915	1333
SBF3	614	616	754	882	984	1267